Cell Reports

Article

cFLIP$_L$ acts as a suppressor of TRAIL- and Fas-initiated inflammation by inhibiting assembly of caspase-8/FADD/RIPK1 NF-κB-activating complexes

Graphical abstract

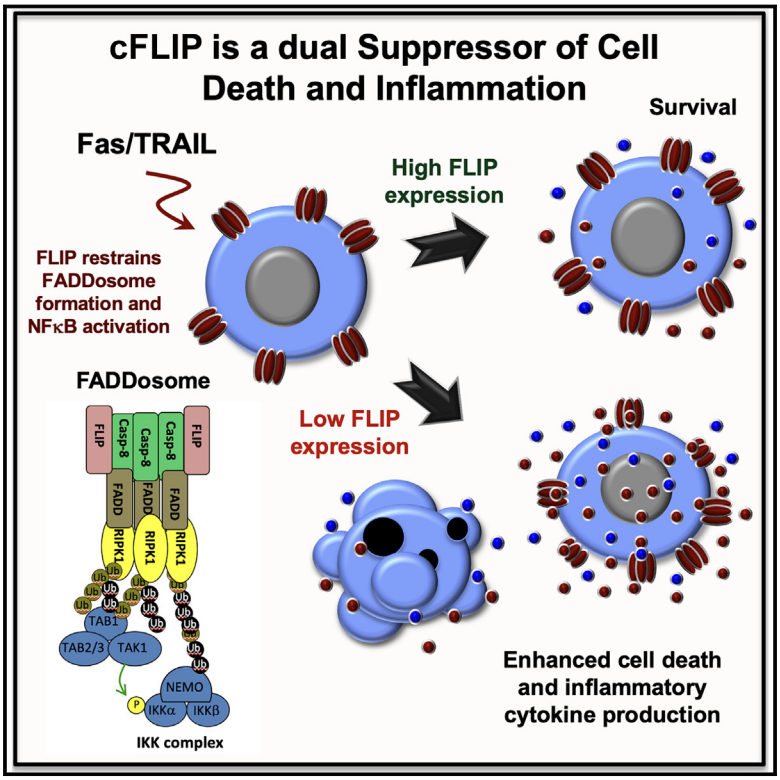

Highlights

- cFLIP suppresses Fas- or TRAIL-induced NF-κB activation and inflammatory cytokine production
- cFLIP inhibits the formation of caspase-8/FADD/RIPK1 NF-κB-activating complexes
- cFLIP inhibits binding of FADD/RIPK1 to FADDosome complexes due to its low affinity for FADD
- cFLIP acts as a bifunctional suppressor of apoptosis and inflammation

Authors

Pavel Davidovich, Catherine A. Higgins, Zaneta Najda, Daniel B. Longley, Seamus J. Martin

Correspondence

martinsj@tcd.ie

In brief

cFLIP is well known to suppress apoptosis initiated through engagement of Fas, TRAIL, or tumor necrosis factor (TNF) "death receptors." Davidovich et al. show that cFLIP also serves as a potent suppressor of Fas- or TRAIL-induced NF-κB activation and inflammatory cytokine production. Thus, cFLIP functions as a dual regulator of apoptosis and inflammation.

Davidovich et al., 2023, Cell Reports *42*, 113476
December 26, 2023
https://doi.org/10.1016/j.celrep.2023.113476

CellPress

Cell Reports

CellPress
OPEN ACCESS

Article

cFLIP$_L$ acts as a suppressor of TRAIL- and Fas-initiated inflammation by inhibiting assembly of caspase-8/FADD/RIPK1 NF-κB-activating complexes

Pavel Davidovich,[1] Catherine A. Higgins,[2] Zaneta Najda,[1] Daniel B. Longley,[2] and Seamus J. Martin[1,3,*]
[1]Molecular Cell Biology Laboratory, Department of Genetics, The Smurfit Institute, Trinity College, Dublin 2, Ireland
[2]Centre for Cancer Research and Cell Biology, Queen's University, Belfast, UK
[3]Lead contact
*Correspondence: martinsj@tcd.ie
https://doi.org/10.1016/j.celrep.2023.113476

SUMMARY

TRAIL and FasL are potent inducers of apoptosis but can also promote inflammation through assembly of cytoplasmic caspase-8/FADD/RIPK1 (FADDosome) complexes, wherein caspase-8 acts as a scaffold to drive FADD/RIPK1-mediated nuclear factor κB (NF-κB) activation. cFLIP is also recruited to FADDosomes and restricts caspase-8 activity and apoptosis, but whether cFLIP also regulates death receptor-initiated inflammation is unclear. Here, we show that silencing or deletion of cFLIP leads to robustly enhanced Fas-, TRAIL-, or TLR3-induced inflammatory cytokine production, which can be uncoupled from the effects of cFLIP on caspase-8 activation and apoptosis. Mechanistically, cFLIP$_L$ suppresses Fas- or TRAIL-initiated NF-κB activation through inhibiting the assembly of caspase-8/FADD/RIPK1 FADDosome complexes, due to the low affinity of cFLIP$_L$ for FADD. Consequently, increased cFLIP$_L$ occupancy of FADDosomes diminishes recruitment of FADD/RIPK1 to caspase-8, thereby suppressing NF-κB activation and inflammatory cytokine production downstream. Thus, cFLIP acts as a dual suppressor of apoptosis and inflammation via distinct modes of action.

INTRODUCTION

Fas and TRAIL receptors are members of the "death receptor" subset of the tumor necrosis factor (TNF) receptor (TNFR) superfamily, which includes TNFR and five other death receptors that can all promote apoptosis under certain conditions.[1–5] Although engagement of Fas or TRAIL receptors with their cognate ligands is well known to promote apoptosis, a number of studies have shown that these receptors can also promote inflammatory cytokine production in multiple contexts.[6–14]

In the context of death receptor signaling, cell death and inflammatory signals typically run in opposition to each other, with more cell death leading to reduced inflammatory cytokine production and vice versa.[6,9,10,15–17] For example, molecules such as inhibitor of apoptosis proteins (IAPs) that promote K63- and M1-linked ubiquitination of RIPK1 and other death receptor components typically suppress cell death and promote inflammation[17]; conversely, inhibition or degradation of IAPs typically leads to increased cell death and reduced inflammation.[17–19] Furthermore, suppression of TRAIL- or Fas-initiated apoptosis through inhibition of caspase activity typically leads to enhanced inflammatory cytokine production through stabilization of the scaffold function of caspase-8 within its associated signaling complexes.[6,9,10]

Engagement of Fas or TRAIL receptors results in the initiation of apoptosis through FADD-dependent recruitment of caspase-8 to the membrane receptor complex, called complex I.[20–24] However, engagement of the latter receptors also results in the assembly of a secondary cytoplasmic complex, presumably due to disengagement of complex I from the receptor, called complex II or the FADDosome.[10,12,25] The FADDosome is composed of the core components caspase-8/FADD/RIPK1 as well as multiple additional constituents, such as cFLIP$_{S/L}$, caspase-10, TRAF2, IAPs, A20, CYLD, NEMO, and other modifiers of cell death or inflammation.[10,11] In contrast to the Fas and TRAIL receptor complexes, caspase-8 is not recruited to the TNFR plasma membrane signaling complex (TNFR complex I), most likely because the latter complex does not recruit FADD.[26,27] Instead, RIPK1 is directly recruited to TNFR complex I via TRADD.[26] Thus, TNFR engagement predominantly promotes RIPK1-dependent inflammatory cytokine production and minimal apoptosis, whereas the reverse is true with respect to Fas and TRAIL receptors.[9,10,27]

Although cytoplasmic caspase-8/FADD/RIPK1 FADDosome complexes can promote caspase-8 processing and activation,[28–30] these complexes also serve a key role in driving RIPK1 ubiquitination to promote NFκB-dependent inflammatory cytokine production, which is critically dependent on the scaffold function of caspase-8 and is enhanced through blocking caspase-8 activity.[6,10,31] cFLIP is very well known to suppress apoptosis through antagonizing the formation of caspase-8/FADD filaments that form downstream of Fas or TRAIL receptor engagement, thereby antagonizing filament-associated caspase-8 homodimerization and full processing and activation of the latter protease.[32–38] cFLIP$_L$ is highly homologous to caspase-8 and is also recruited to Fas and TRAIL-induced complex I, as well as the cytoplasmic

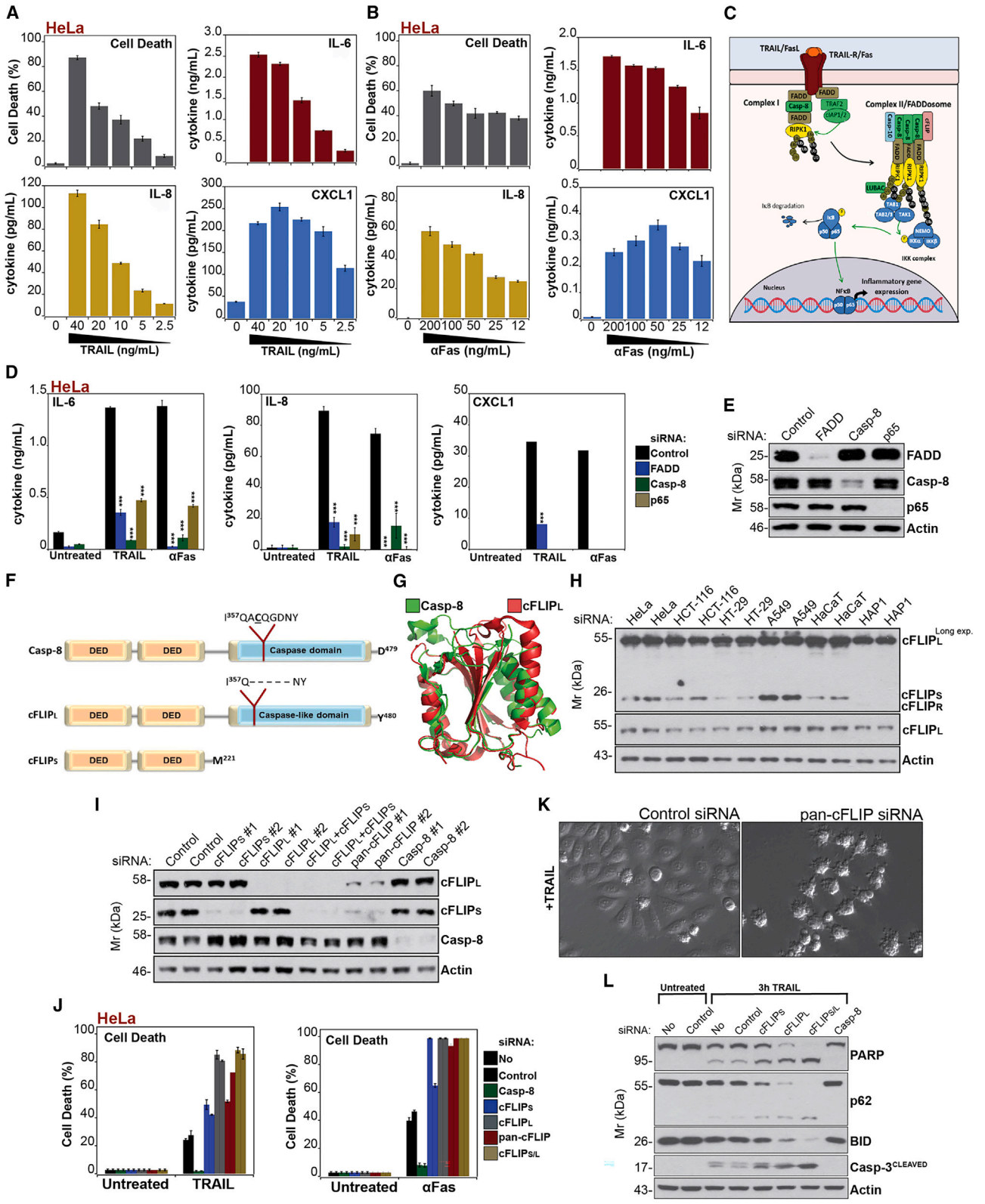

(legend on next page)

FADDosome complex,[8,10,25] possibly through direct binding to FADD via DED-DED interactions with the latter,[39–41] or more likely through heterodimerization with caspase-8.[10,36–38] However, it is unclear whether cFLIP also regulates FADDosome-mediated inflammatory cytokine production, either through competing with caspase-8 to form $cFLIP_L$/FADD/RIPK1 complexes, given the high degree of homology between $cFLIP_L$ and caspase-8, or through restricting the processing and activation of caspase-8 within the complex. Previous studies on the impact of cFLIP on nuclear factor κB (NF-κB) activation have produced opposing conclusions, with some studies suggesting that cFLIP isoforms can activate NF-κB,[42–45] while other data suggest an inhibitory role.[6,8,46] Irrespective of the positive or negative impact of cFLIP on NF-κB activation, how the latter pseudocaspase regulates inflammatory signaling remains obscure.

Here, we explore the role of cFLIP in regulating inflammatory outcomes of Fas and TRAIL receptor engagement and show that $cFLIP_L$ acts as a potent suppressor of inflammation, as well as cell death, which runs counter to the paradigm that suppressors of cell death typically enhance inflammation. Silencing of $cFLIP_L$ expression led to enhanced Fas- or TRAIL-induced cell death as expected but also to greatly enhanced production of multiple pro-inflammatory cytokines, contrary to expectation. We found that $cFLIP_L$ suppressed death receptor-initiated inflammation through antagonizing the assembly of cytoplasmic caspase-8/FADD/RIPK1 complexes (i.e., FADDosomes or complex II), thereby antagonizing RIPK1-driven NF-κB and $p38^{MAPK}$ activation downstream. Thus, in addition to its well-known role as a key arbiter of death receptor-initiated cell death outcomes, $cFLIP_L$ also serves as a potent suppressor of inflammation through limiting the recruitment of FADD/RIPK1 to caspase-8-associated cytoplasmic signaling complexes formed upon engagement of these receptors.

RESULTS

TRAIL and Fas stimulation promotes cell death as well as inflammation

As shown in Figures 1A and 1B, stimulation of HeLa cells with TRAIL or cross-linking anti-Fas antibodies triggered extensive apoptosis, as expected. Moreover, Fas or TRAIL-stimulated cells also secreted a range of pro-inflammatory cytokines and chemokines, including interleukin (IL)-6, IL-8, and CXCL1 (Figures 1A and 1B), as previously reported.[6,8–11] Similarly, Fas or TRAIL stimulation induced cell death and inflammatory cytokine production in multiple other cell types (Figures S1A–S1D). We have previously reported that caspase-8 plays an indispensable, non-enzymatic, role as a scaffold in the formation of cytoplasmic caspase-8/FADD/RIPK1 complexes (FADDosomes), which are instrumental in Fas- or TRAIL-induced cytokine production[10] (Figure 1C). Consistent with this, knockdown of caspase-8 or FADD resulted in essentially complete suppression of Fas- or TRAIL-induced IL-6, IL-8, and CXCL1 production (Figures 1D and 1E).

Caspase-8 is highly homologous with $cFLIP_L$, a non-enzymatically active pseudocaspase that is the major suppressor of death receptor-initiated cell death (Figures 1F and 1G). A shorter splice variant, $cFLIP_S$, can also suppress death receptor-initiated cell death, although the longer splice variant, $cFLIP_L$, is typically much more abundantly expressed in many commonly used cell lines (Figure 1H). $cFLIP_L$ suppresses death receptor-initiated apoptosis through forming heterodimers with caspase-8 and restricting the protease activity of the latter, as well as accelerating caspase-8 processing,[36,47] and, in the case of $cFLIP_S$, through terminating the formation of caspase-8 oligomers downstream of death receptor engagement.[34] However, the impact of cFLIP on death receptor-initiated cytokine production has not been explored in depth and, indeed, whether cFLIP promotes or inhibits NF-κB activation is controversial.[6,8,42–46] To address this issue, we designed small interfering RNAs (siRNAs) specific for $cFLIP_L$, $cFLIP_S$, or targeted against both cFLIP isoforms (Figures 1I and S1E). Individual cFLIP isoforms were efficiently silenced with their respective siRNAs (Figure 1I) and knockdown of either or both isoforms greatly sensitized HeLa cells to TRAIL- or Fas-induced apoptosis (Figures 1J–1L), as expected.

Silencing of $cFLIP_L$ expression enhances TRAIL- or Fas-initiated inflammation

As noted earlier, cell death and inflammatory signals typically run counter to each other downstream of death receptor engagement, with perturbations that increase cell death (such as inhibition of IAPs or A20) leading to a reduction in inflammatory

Figure 1. TRAIL and Fas receptor engagement initiates caspase-8-dependent cell death and cytokine secretion

(A and B) HeLa cells were stimulated with the indicated concentrations of TRAIL or anti-Fas immunoglobulin (Ig) M (CH11) for 24 h, followed by assessment of apoptosis based on cell morphology on counts of triplicate fields of ~100 cells (a minimum of 300 cells per well). Cytokine concentrations in cell culture supernatants were determined by ELISA.

(C) Schematic representation of NF-κB activation via the caspase-8/FADD/RIPK1 FADDosome complex.

(D and E) HeLa cells were nucleofected with non-targeting siRNA (control oligo) or two independent siRNAs specific for FADD, caspase-8, or NF-κB p65. After 48 h, cells were either left untreated or treated with TRAIL or anti-Fas for a further 24 h before cytokine determination by ELISA. Knockdown efficiency and specificity of the indicated siRNAs as assessed by western blotting.

(F) Schematic representation of caspase-8, $cFLIP_L$, and $cFLIP_S$ domain structures.

(G) Structural alignment of caspase-8 and $cFLIP_L$.

(H) $cFLIP_L$ and $cFLIP_S$ expression levels in the indicated cell lines was assessed by western blotting.

(I) HeLa cells were nucleofected with either non-targeting siRNA (control oligo) or siRNAs targeted against the indicated gene products and knockdown efficiency assessed by western blotting after 48 h.

(J) HeLa cells were nucleofected with the indicated siRNAs for 48 h followed by treatment with either TRAIL or anti-Fas for a further 18 h and assessment of cell death.

(K and L) HeLa cells were nucleofected with the indicated siRNAs and, 48 h later, were treated TRAIL. After 6 h of TRAIL treatment, representative phase contrast images were taken (K) and cell lysates were analyzed for apoptosis markers and caspase substrates by western blotting (L). Error bars are the mean ± SEM of triplicate determinations from representative experiments. Significance levels: ***$p < 0.0001$, **$p < 0.001$, *$p < 0.01$ by Student's t test. In all cases, results shown are representative of three independent experiments. See also Figure S1.

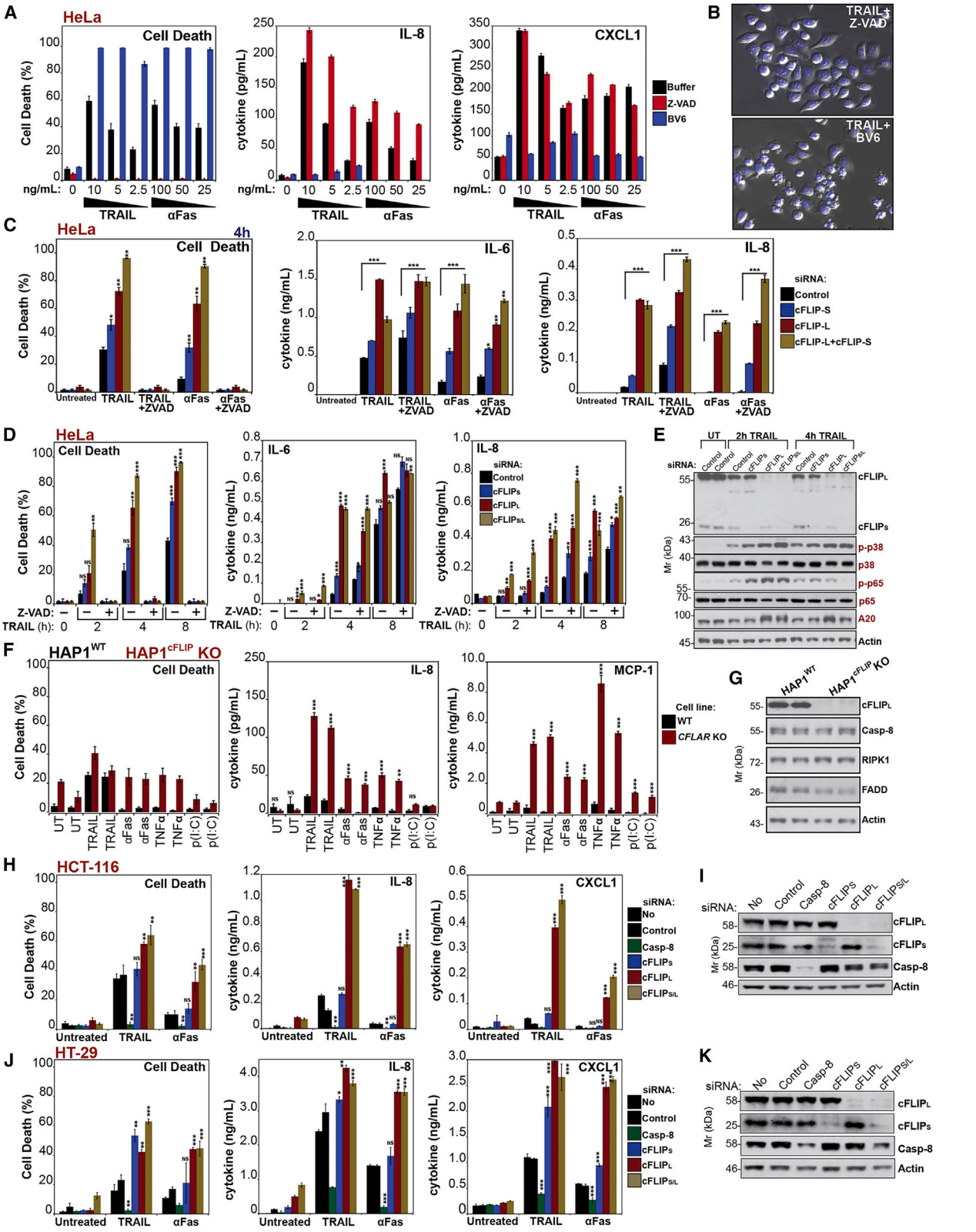

(legend on next page)

cytokine production[17–19] and perturbations that suppress cell death (such as caspase inhibition) resulting in enhanced inflammatory cytokine production.[4,10] Indeed, as Figures 2A and 2B illustrate, although TRAIL- and Fas-induced cell death were blocked by the poly-caspase inhibitor Z-VAD-FMK, the production of inflammatory cytokines by Fas or TRAIL stimulation was enhanced under the same conditions. In contrast, the IAP antagonist BV6 robustly enhanced cell death in response to Fas or TRAIL but suppressed TRAIL- and Fas-induced cytokine production under the same conditions (Figures 2A and 2B).

We next explored the effects of cFLIP silencing on Fas- and TRAIL-induced cytokine production. As expected, knockdown of $cFLIP_L$, or $cFLIP_S$ to a lesser degree, led to enhanced cell death in response to Fas or TRAIL receptor engagement (Figures 2C–2E). However, in sharp contrast to the reciprocal relationship typically seen between cell death and inflammatory outcomes (Figure 2A), knockdown of $FLIP_L$, as well as $cFLIP_S$ to a lesser degree, led to robustly *enhanced* cytokine production in tandem with enhanced cell death, in response to Fas or TRAIL treatment (Figures 2C–2E and S2A–S2D). Importantly, we also observed a similarly robust increase in cytokine production in cFLIP/*CFLAR*-knockout HAP1 cells (Figures 2F and 2G), as well as upon silencing of $cFLIP_L$ in multiple additional cell types, including HCT-116, HT-29, A549, and HaCaT cells (Figures 2H–2K and S2E–S2H), which again ran counter to the effects of caspase-8 knockdown in the latter cells. Given the structural similarity between caspase-8 and $cFLIP_L$ (Figures 1F and 1G), and the fact that the catalytic activity of caspase-8 is not required for the pro-inflammatory activity of caspase-8/FADD/RIPK1 FADDosomes,[10] the diametrically opposed effects of silencing caspase-8 (Figures 1D and S2B) or $cFLIP_L$ (Figures 2C, 2D, and S2B) on inflammatory outputs was surprising. These data suggest that, in addition to its role as a key arbiter of death receptor-initiated apoptosis, $cFLIP_L$ also acts as a potent suppressor of death receptor-driven inflammation.

The effects of $cFLIP_L$ loss on inflammatory outcomes is unrelated to its effects on caspase-8 activity and apoptosis

One possibility was that the increased cell death observed upon silencing of $cFLIP_L$ expression led to enhanced cytokine production due to an increase in the passive release of cytokines from dying cells. However, silencing of $cFLIP_L$ in the presence of caspase inhibitors (to block cell death) still resulted in a dramatic enhancement of TRAIL- or Fas-induced cytokine production (Figures 3A and 3B and S3A), demonstrating that the role of $cFLIP_L$ in regulating inflammatory cytokine production was unrelated to its effects on caspase-8 activation and cell death. Because RIPK1 is a substrate for caspase-8,[48] an additional possibility was that caspase-8:$cFLIP_L$ heterodimers cleaved RIPK1 more efficiently than caspase-8 homodimers,[34,49] thereby inhibiting RIPK1-mediated NF-κB activation as a consequence of increased proteolysis of RIPK1. However, at odds with this possibility, RIPK1 was cleaved *more* efficiently upon knockdown of $cFLIP_L$ (Figures 3C and 3D). The latter observation ruled out the possibility that reduced caspase-8-mediated proteolysis of RIPK1 was responsible for the increase in cytokine production observed in the absence of $cFLIP_L$. Furthermore, assessment of early signal transduction events seen in response to TRAIL or Fas stimulation revealed that phosphorylation of NF-κB p65 as well as $p38^{MAPK}$, both of which are required for Fas- and TRAIL-induced cytokine production,[9,10] were robustly enhanced upon silencing of $cFLIP_L$ expression (Figures 3C and 3D). Similar observations were also made in FLIP/*CFLAR*-knockout HAP1 cells (Figure 3E). $cFLIP_L$ silencing also led to enhanced TRAIL- or Fas-induced expression of IL-6 and IL-8 mRNA (Figures 3F and 3G), as well as enhanced cytokine secretion at very early time points after TRAIL or Fas stimulation (Figure 3H), when enhancement of cell death due to $cFLIP_L$ silencing was not yet significant.

Although overexpression of cFLIP can produce complex effects, we also explored the impact of transfecting plasmids encoding $cFLIP_L$, as well as the viral FLIP variants vFLIP-MC159 and vFLIP-MC160, on cytokine production initiated by a catalytically

Figure 2. Silencing of $cFLIP_L$ expression enhances TRAIL- and Fas-induced inflammatory cytokine production

(A) HeLa cells were pre-treated for 2 h with the IAP antagonist BV6 (1 μM) or the poly-caspase inhibitor Z-VAD-FMK (10 μM), followed by treatment with TRAIL or anti-Fas IgM. After 18 h, apoptosis was assessed on counts of triplicate fields of at least 100 cells and cytokine concentrations in culture supernatants were determined by ELISA.

(B) Phase contrast images of HeLa cells treated for 18 h, as indicated, followed by staining with DNA-binding dye DAPI.

(C) HeLa cells were nucleofected with the indicated siRNAs against cFLIP isoforms and, 48 h later, were treated with either TRAIL or anti-Fas for a further 4 h in presence or absence of 10 μM poly-caspase inhibitor Z-VAD-FMK. Apoptosis was assessed based on cell morphology on counts of triplicate fields of at least 100 cells and cytokine concentrations in culture supernatants were determined by ELISA.

(D) HeLa cells were nucleofected with the indicated siRNAs against cFLIP isoforms and, 48 h later, were treated with TRAIL in presence or absence of 10 μM Z-VAD-FMK for 18 h. Apoptosis was assessed based on cell morphology on counts of triplicate fields of at least 100 cells and cytokine concentrations in culture supernatants were determined by ELISA.

(E) Knockdown efficiency of cells treated as in (D) and inflammatory markers were assessed by western blotting.

(F) WT and $cFLIP^{KO}$ HAP1 cells were either left untreated (UT) or were incubated with TRAIL (100, 50 ng/mL), anti-Fas (400, 200 ng/mL), TNFα (2, 1 ng/mL), or poly(IC) (40, 20 μg/mL) for 20 h, followed by measurement of apoptosis based on cell morphology on counts of triplicate fields of at least 100 cells, and measurement of cytokine concentrations in culture supernatants by ELISA.

(G) WT and $cFLIP^{KO}$ HAP1 cells were immunoblotted for the indicated proteins.

(H and J) HCT-116 and HT-29 cells were nucleofected with the indicated siRNAs and, 48 h later, were treated with either TRAIL or anti-Fas for a further 18 h. Apoptosis was assessed based on cell morphology on counts of triplicate fields of at least 100 cells and cytokine concentrations in culture supernatants were determined by ELISA.

(I and K) Knockdown efficiency of the siRNAs used in (H) and (J) were validated by western blot. Error bars represent the mean ± SEM of triplicate cell counts from representative experiments. In all cases, results shown are representative of three independent experiments. Significance levels: ***$p < 0.0001$, **$p < 0.001$, *$p < 0.01$ by Student's t test. See also Figure S2.

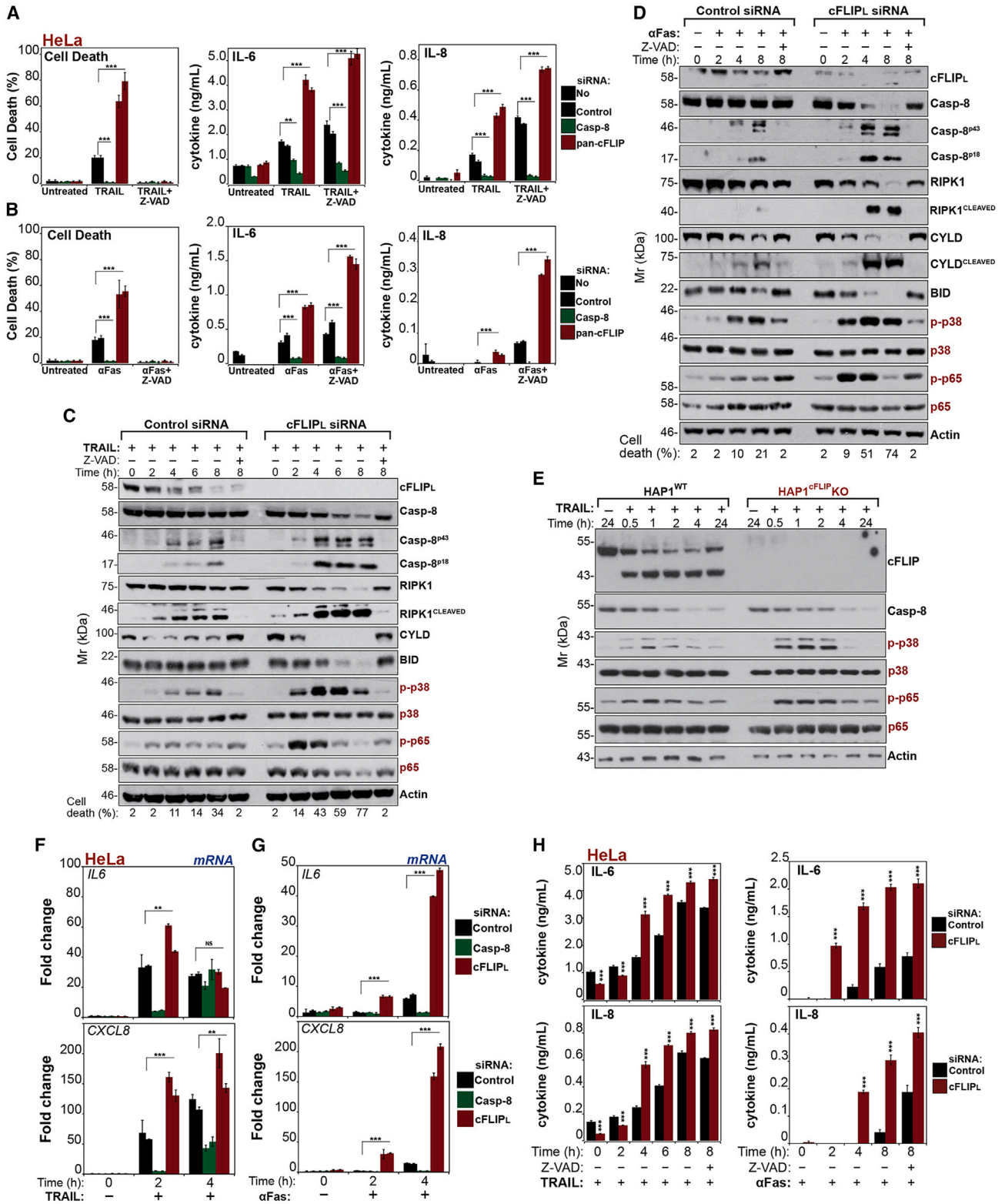

(legend on next page)

inactive caspase-8 mutant (C360A). The latter caspase-8 mutant serves as a scaffold to promote robust RIPK1-dependent inflammatory cytokine production upon transient overexpression.[10] As Figures S3B and S3C illustrate, while overexpression of the caspase-8 catalytically inactive mutant induced robust cytokine production, neither cFLIP$_L$ nor either vFLIP variant promoted cytokine production. Moreover, co-expression of cFLIP$_L$ or either vFLIP variant suppressed IL-8 production driven by the catalytically inactive caspase-8 mutant (Figure S3B).

Collectively, the preceding data suggested that deletion or silencing of cFLIP$_L$ led to more efficient engagement of death receptor signaling complexes, resulting in enhanced NF-κB and p38^{MAPK} activation and inflammatory cytokine production downstream, unrelated to increases in cell death or caspase-8 activity observed under the same conditions.

The enhanced cytokine production observed upon cFLIP$_L$ loss is dependent on FADD, caspase-8, and RIPK1

Formation of cytosolic caspase-8/FADD/RIPK1 complexes plays a key role in promoting NFκB-dependent cytokine production in response to TRAIL- or Fas-stimulation[10] (Figures 1C and 1D). Consistent with this, knockdown of FADD or caspase-8 in combination with cFLIP$_L$ reversed the enhanced cytokine production seen upon knockdown of cFLIP$_L$ alone (Figures 4A and 4B). Furthermore, combined knockdown of RIPK1 and TAK1 suppressed inflammatory cytokine production in response to Fas or TRAIL receptor stimulation (Figures 4C–4F). To confirm that the enhanced inflammation observed in the absence of cFLIP$_L$ was RIPK1 dependent, we silenced cFLIP$_L$ either alone or in combination with RIPK1 and/or TAK1. As Figures 4E–4G shows, knockdown of RIPK1 in combination with cFLIP$_L$ reversed the enhanced cytokine production seen upon silencing of cFLIP$_L$ alone, which was further suppressed upon silencing of TAK in combination with RIPK1. These data argue that cFLIP regulates death receptor-initiated inflammation via the caspase-8/FADD/RIPK1 FADDosome complex.

cFLIP$_L$ also plays a role in suppressing TLR3-mediated inflammation

TLR3 can also promote apoptosis and inflammation through assembly of a TRIF-RIPK1-FADD-caspase-8 complex.[30] Therefore, we also explored whether TLR3-mediated apoptosis and inflammation could be regulated by cFLIP$_L$. As Figure S4A illustrates, treatment of HeLa cells with the TLR3 ligand poly(IC) resulted in apoptosis as well as the production of inflammatory cytokines. Furthermore, knockdown of cFLIP$_L$ resulted in enhancement of poly(IC)-induced cell death as well as IL-6 and IL-8 production (Figure S4B), similar to the pattern observed with Fas or TRAIL stimulation. Moreover, the enhancement of poly(IC)-induced cytokine production seen upon silencing of cFLIP$_L$ was reversed upon knockdown of caspase-8 or FADD in combination with cFLIP$_L$, consistent with a role for the FADDosome in driving inflammatory cytokine production in this context (Figure S4C). Similar to what we observed with TRAIL or Fas (Figures 3A and 3B), suppression of poly(IC)-induced cell death with Z-VAD-FMK still led to enhanced cytokine production upon knockdown of cFLIP$_L$ (Figure S4D), once again suggesting that the effect of cFLIP$_L$ on inflammatory cytokine production was independent of its role in regulating caspase-8 activation or cell death outcomes. Of note, cytokine production in response to poly(IC) was independent of TNF production, as inclusion of a TNF-neutralizing antibody (Figure S4E) had no effect on poly(IC)-induced cell death or cytokine production in this context (Figure S4F).

cFLIP$_L$ loss results in enhanced recruitment of RIPK1 into higher-molecular-weight signaling complexes

To explore the effects of cFLIP$_L$ loss on the recruitment of RIPK1 into the signaling complexes involved in Fas- and TRAIL-initiated cytokine production, we initially investigated this using DSS-induced cross-linking in cell lysates from control versus cFLIP$_L$ silenced cells. As Figure 4H demonstrates, in response to TRAIL stimulation, RIPK1 underwent a shift into higher-molecular-weight complexes, which were revealed by DSS-mediated cross-linking. Furthermore, upon silencing of cFLIP$_L$, expression, RIPK1 incorporation into higher-molecular-weight complexes was enhanced (Figures 4I–4K). These data suggest that RIPK1 was more efficiently incorporated into signaling complexes in the absence of cFLIP$_L$, resulting in enhanced RIPK1-dependent cytokine production.

RIPK1 recruitment and ubiquitination within cytosolic FADDosome complexes is enhanced in the absence of cFLIP$_L$

We next explored the effects of cFLIP$_L$ silencing on recruitment of effector molecules into plasma-membrane-associated (Figures 5A and 5B), versus cytosolic (Figures 5C and 5D), death receptor-induced signaling complexes. As expected, TRAIL-induced

Figure 3. Enhanced inflammatory signaling due to loss of cFLIP$_L$ can be uncoupled from cell death outcomes

(A and B) HeLa cells were nucleofected with the indicated siRNAs and, 48 h later, cells were treated with either TRAIL or anti-Fas for a further 18 h in the presence or absence of Z-VAD-FMK (10 μM), as indicated. Apoptosis was assessed by morphology on triplicate fields of at least 100 cells per field and cytokine concentrations in culture supernatants were determined by ELISA.

(C and D) HeLa cells were nucleofected with non-targeting (control) or cFLIP$_L$-specific siRNAs and, 48 h later, were treated with TRAIL (5 ng/mL) or anti-Fas (50 ng/mL) in the presence or absence of Z-VAD-FMK (10 μM) for the indicated times. Cell lysates were immunoblotted for the indicated cell death or inflammatory signaling proteins and apoptosis was assessed (based on cell morphology) on counts of triplicate fields of at least 100 cells.

(E) HAP1 WT and HAP1 *CFLAR* null cells were treated with TRAIL (200 ng/mL) for the indicated times and cell lysates were immunoblotted for the indicated proteins.

(F and G) HeLa cells were nucleofected with the indicated siRNAs and, 48 h later, were treated with either anti-Fas or TRAIL for the indicated times, followed by quantitation of *IL6* and *CXCL8* mRNAs by qPCR.

(H) HeLa cells were nucleofected with either non-targeting oligo (control) or cFLIP$_L$-targeting siRNAs and, 48 h later, cells were treated with either TRAIL or anti-Fas, in the presence or absence of Z-VAD-FMK (10 μM), for the indicated times. Cytokine concentrations in culture supernatants were determined by ELISA. Results shown are representative of least three independent experiments. Error bars represent the mean ± SEM of triplicate determinations from a representative experiment. Significance levels: ***p < 0.0001, **p < 0.001, *p < 0.01 by Student's t test. See also Figure S3.

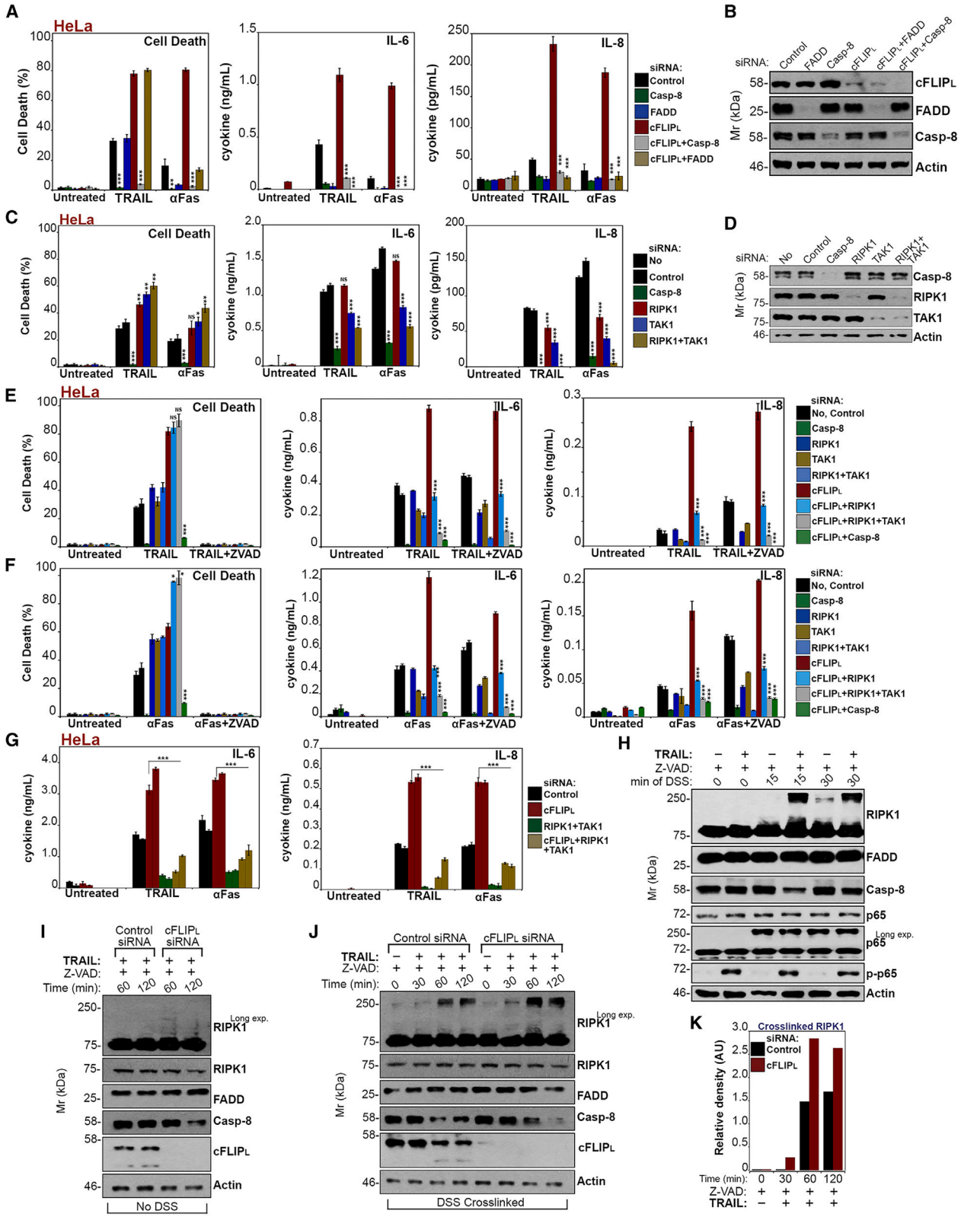

(legend on next page)

membrane-associated receptor complexes (complex I) contained FADD, caspase-8, cFLIP, and traces of RIPK1 and caspase-10 (Figure 5B). However, cytoplasmic TRAIL-induced FADDosome complexes (complex II) contained robust amounts of RIPK1 in addition to caspase-8 and FADD (Figures 5C and 5D). $cFLIP_L$ was also recruited into the latter complexes, along with other constituents such as caspase-10, A20, and other downstream regulators of NF-κB activation[10] (Figures 5D, S5A, and S5B). To explore the effects of $cFLIP_L$ loss on recruitment of RIPK1 into cytoplasmic FADDosome complexes further, we immunoprecipitated caspase-8 from HeLa cells at various times after Fas or TRAIL stimulation and assessed the effects of $cFLIP_L$ knockdown on the recruitment of FADD and RIPK1, as well as other signaling constituents, into these complexes. As Figures 5E–5G, S5C, and S5D illustrate, silencing of $cFLIP_L$ expression resulted in enhancement of RIPK1 and FADD recruitment into FADDosome complexes, along with increased TRAF2 and A20 recruitment, as expected. Furthermore, immunoprecipitation (IP) of membrane TRAIL receptor complexes in the presence or absence of $cFLIP_L$ revealed that recruitment of FADD and RIPK1 to these complexes was also enhanced upon silencing of $cFLIP_L$ expression (Figures 6A and 6B), again suggesting that $cFLIP_L$ restrains recruitment of FADD, and in turn RIPK1, to caspase-8. Highly similar observations were made when comparing TRAIL-R2 complexes immunoprecipitated from TRAIL-treated wild-type (WT) versus cFLIP/*CFLAR*-knockout HAP1 cells (Figure 6C).

Previous studies have shown that RIPK1 activation within death receptor signaling complexes is associated with multiple ubiquitin modifications of RIPK1, including linear Ub chains and K63-Ub chains, which facilitate recruitment of downstream signaling molecules, such as IKKγ/NEMO as well as the TAB/TAK complex, that promote NF-κB activation downstream.[5,12] Consistent with the enhanced cytokine production observed in the absence of $cFLIP_L$ (Figure 2), we also observed enhanced RIPK1 ubiquitination, enhanced recruitment of the LUBAC complex catalytic subunit HOIP, as well as enhanced recruitment of A20, TBK1, and NEMO to FADDosome complexes upon silencing of $cFLIP_L$ (Figures 6D and 6E).

$cFLIP_L$ has a low affinity for FADD, as compared with caspase-8, thereby restricting recruitment of FADD and RIPK1 to FADDosomes

Interestingly, we observed greatly enhanced recruitment of caspase-10 (Figures 5E and 5F) into FADDosome complexes upon knockdown of $cFLIP_L$. Because a previous study has implicated caspase-10 as a driver of NF-κB activation downstream of death receptor engagement,[50] this suggested the possibility that enhanced caspase-10 recruitment into the latter complexes might be responsible for the enhanced cytokine production seen in the absence of $cFLIP_L$. To explore this possibility, we silenced caspase-10 expression either alone or in combination with $cFLIP_L$ and assessed the impact of this on Fas- or TRAIL-induced cytokine production. However, as Figures 7A and 7B illustrate, silencing of caspase-10 expression had no impact on death receptor-induced cytokine production in the presence or absence of $cFLIP_L$, ruling out a role for caspase-10 as a key regulator of cytokine production in this context. We also saw enhanced recruitment of TRAF2 into FADDosome complexes upon silencing of $cFLIP_L$ (Figures 5E and 5F). Thus, we also explored the effects of $cFLIP_L$ knockdown, alone or in combination with TRAF2, to ask whether silencing of TRAF2 reversed the enhanced inflammation seen upon $cFLIP_L$ knockdown. However, as Figures 7C and 7D illustrate, TRAF2 silencing was not sufficient to reverse the effects of $cFLIP_L$ knockdown on cytokine production, although a caveat to the latter conclusion is that knockdown of TRAF2 was not complete. Because TRAF2 typically recruits IAPs to death receptor complexes, we also explored the effects of the IAP antagonist BV6 on the enhanced inflammation observed upon $cFLIP_L$ silencing. As Figure S6 illustrates, addition of BV6 completely suppressed the enhanced inflammation associated with $cFLIP_L$ knockdown, as expected.

The preceding data indicated that $cFLIP_L$ suppressed the formation of FADDosome complexes as well as the recruitment of downstream signaling constituents to these complexes. This suggested that, although caspase-8 binds FADD efficiently, which in turn recruits RIPK1 to the complex, $cFLIP_L$ has a reduced affinity for FADD, thereby resulting in diminished RIPK1 recruitment and formation of caspase-8/FADD/RIPK1 signaling complexes (i.e., FADDosomes) when $cFLIP_L$ is abundant. To explore this further, we examined the recruitment of FADD, $cFLIP_L$, and RIPK1 to TRAIL-R2 membrane receptor complexes in WT versus *CASP-8* null HeLa cells. As previously reported,[10] TRAIL- and Fas-induced apoptosis, as well as inflammatory cytokine production, were completely suppressed in cells lacking *CASP-8* (Figures 7E and 7F), despite the presence of caspase-10 in these cells (Figure 7B). Furthermore, IP of TRAIL receptor complexes in WT versus *CASP-8* null cells revealed that FADD and $cFLIP_L$ failed to be recruited to the

Figure 4. $cFLIP_L$ silencing promotes caspase-8/FADD/RIPK1-dependent inflammation

(A and C) HeLa cells were nucleofected with the indicated siRNAs and, 48 h later, were treated with either TRAIL or anti-Fas for a further 18 h. Apoptosis was assessed by morphology on triplicate fields of at least 100 cells per field; cytokine concentrations in culture supernatants were determined by ELISA.

(B, D) Knockdown efficiency in A and C was validated by immunoblotting.

(E–G) HeLa cells were nucleofected with the indicated siRNAs and, 48 h later, cells were treated with either TRAIL or anti-Fas for a further 18 h. Apoptosis was assessed by morphology on triplicate fields of at least 100 cells per field; cytokine concentrations in culture supernatants were determined by ELISA.

(H) HeLa cells (6×10^6 per treatment) were stimulated with TRAIL for 2 h in the presence of Z-VAD-FMK (10 μM). Cells were then lysed and incubated in the presence or absence of DSS cross-linking reagent for the indicated times, followed by analysis by western blotting.

(I and J) HeLa cells were nucleofected with either non-targeting siRNA or $cFLIP_L$-specific siRNAs and, 48 h later, cells were treated with TRAIL in the presence of Z-VAD-FMK (10 μM) for the indicated times. Cells were then lysed in the presence or absence of DSS crosslinker, as indicated, followed by analysis of the FADDosome proteins by immunoblotting.

(K) Densitometry analysis of high-molecular-weight adducts of RIPK1 from (J). Results shown are representative of least three independent experiments. Error bars represent the mean ± SEM of triplicate cell counts from a representative experiment. Significance levels: ***$p < 0.0001$, **$p < 0.001$, *$p < 0.01$, by Student's t test. See also Figure S4.

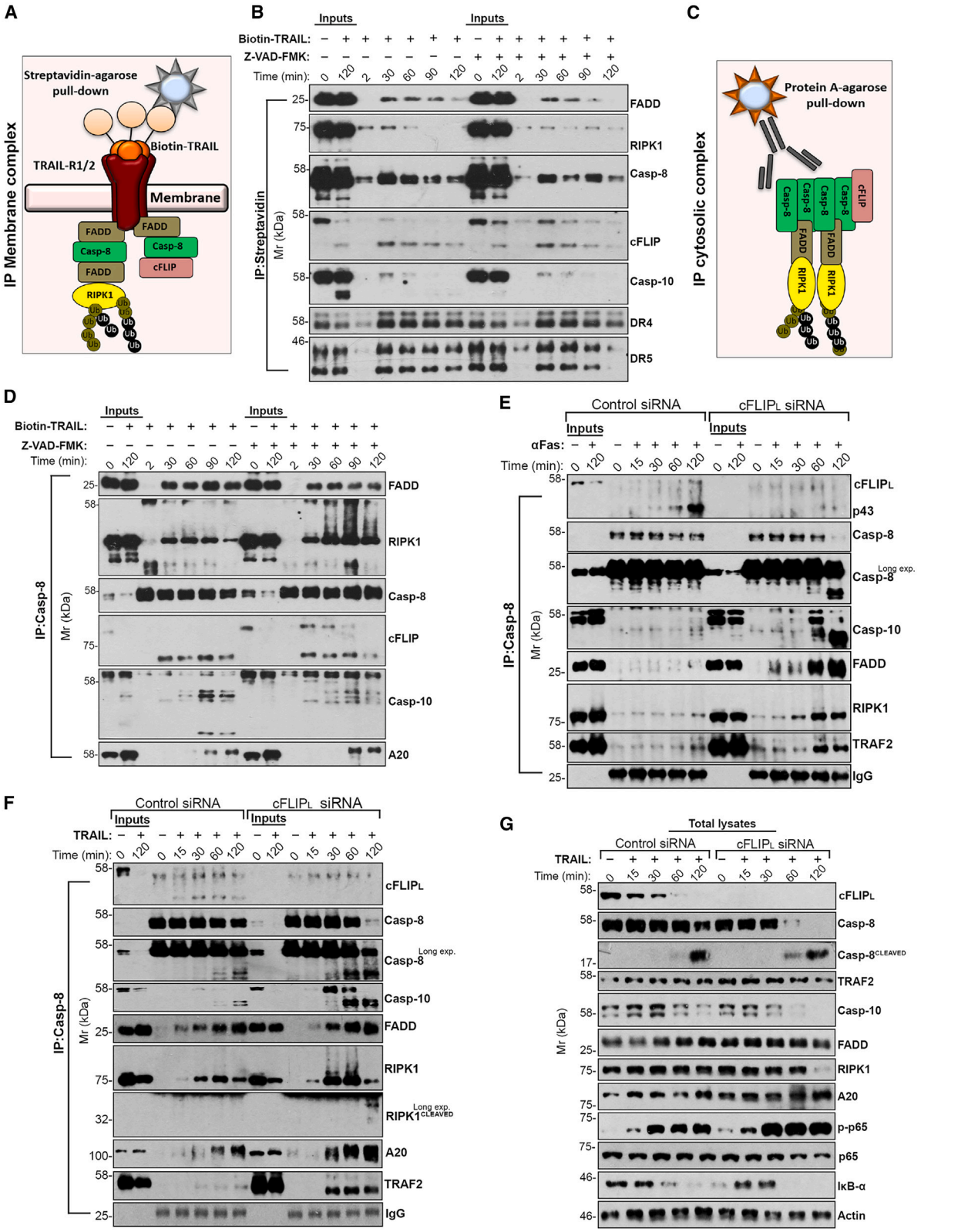

(legend on next page)

receptor complex in cells deficient in *CASP-8* (Figures 7G and 7H), demonstrating that caspase-8 serves as an essential scaffold for recruitment of cFLIP and FADD to the membrane receptor complex. To further explore the relative affinity of caspase-8 and cFLIP$_L$ for binding to FADD, we also carried out pull-down assays using glutathione S-transferase (GST)-FADD versus *in vitro* transcribed/translated ^{35}S-labeled caspase-8 or ^{35}S-cFLIP$_L$, either alone or in combination. As Figure 7I illustrates, although ^{35}S-caspase-8 efficiently bound to GST-FADD, ^{35}S-cFLIP$_L$ was not captured under the same conditions. However, introduction of both proteins led to capture of ^{35}S-cFLIP$_L$ by GST-FADD (Figure 7I). This again suggested that caspase-8 and cFLIP$_L$ bind in a hierarchical manner to FADD, with caspase-8 binding efficiently to the latter, leading to recruitment of cFLIP$_L$ via heterodimerization with caspase-8 (rather than through direct binding of cFLIP$_L$ to FADD).

Taken together, the foregoing data suggest that cFLIP$_L$ suppresses the formation of caspase-8/FADD/RIPK1 complexes due to the reduced affinity of cFLIP$_L$ for FADD, as compared with the high affinity of caspase-8 for the latter. Thus, cFLIP$_L$ is a potent suppressor of inflammatory signaling in multiple contexts through restricting RIPK1 recruitment to the associated signaling complexes. In addition to the well-established role for cFLIP$_L$ as an inhibitor of apoptosis through diminishing the catalytic activity of caspase-8 toward pro-apoptotic substrates, such as Bid and caspase-3, cFLIP$_L$ also suppresses the inflammatory output of death receptor complexes through attenuating the assembly of FADDosome complexes, thereby diminishing RIPK1/TAK1-mediated NF-κB and p38^{MAPK} activation downstream (Figure 7J).

DISCUSSION

Here, we have shown that cFLIP$_L$ acts as a potent suppressor of inflammation in the context of TRAIL, Fas, or TLR3 receptor engagement. Although cFLIP$_L$ suppresses apoptosis through limiting the formation of fully active caspase-8 homodimers downstream of receptor engagement,[33,36] cFLIP$_L$ suppressed the inflammatory output of death receptors through limiting the formation of cytoplasmic caspase-8/FADD/RIPK1 (FADDosome) complexes due to the greatly reduced affinity of cFLIP$_L$ for FADD (which recruits RIPK1). Thus, FADDosome complexes containing high levels of cFLIP$_L$ have reduced levels of FADD/RIPK1, thereby leading to diminished RIPK1-dependent cytokine production downstream.

Although cFLIP has long been known to inhibit apoptosis,[32,51] how the two main cFLIP isoforms suppress apoptosis has been debated, with initial proposals suggesting that cFLIP isoforms compete with caspase-8 for binding to FADD via DED-DED interactions.[32,51] However, more recent observations suggest that the DEDs of caspase-8 have a much greater affinity for FADD than does the corresponding DED of cFLIP.[10,36,41] Thus, the primary mechanism of inhibition of apoptosis by cFLIP$_L$ is through binding of the latter to caspase-8 to form caspase-8:cFLIP$_L$ heterodimers that possess restricted protease activity or, in the case of cFLIP$_S$, via terminating the formation of tandem caspase-8:caspase-8 polymeric chains/filaments that propagate capase-8 activation downstream of receptor complex formation.[36–38] In accordance with this, formation TRAIL or Fas receptor complexes in *CASP-8* null cells is greatly impaired, despite abundant cFLIP and caspase-10 in such cells that could, in principle, bind to FADD in complexes lacking caspase-8.[10,41] Collectively, the available data indicate that the hierarchy of binding to FADD downstream of TRAIL and Fas receptor stimulation is caspase-8, followed by cFLIP$_L$, followed by caspase-10.[10,34,50] Where caspase-8 is not present, cFLIP$_L$ and caspase-10 binding to FADD is essentially abolished[10,41] (shown in this study). Furthermore, upon experimental depletion of cFLIP$_L$, robust increases in caspase-10 and TRAF2 recruitment to caspase-8 is observed[8] (also shown in this study). Thus, the primary driver of RIPK1 recruitment to TRAIL- or Fas-initiated signaling complexes is caspase-8 through further binding of FADD-RIPK1 to caspase-8 chains that are formed downstream of initial receptor assembly (Figure 1C). Similarly, upon assembly of cytoplasmic caspase-8/FADD/RIPK1 FADDosome complexes that promote NF-κB activation, recruitment of cFLIP$_L$ to caspase-8 within the latter complexes diminishes further FADD and RIPK1 recruitment due to the weak affinity of cFLIP$_L$ for FADD. An alternative explanation is that high levels of cFLIP$_L$ suppress the formation of cytoplasmic caspase-8/FADD/RIPK1 FADDosome complexes *de novo*, rather than FADD/RIPK1 recruitment to these complexes (Figure 7J).

Paradoxically, several studies have shown that formation of caspase-8:cFLIP$_L$ heterodimers result in accelerated caspase-8 processing, as compared with caspase-8 homodimers.[36,41] However, although the kinetics of caspase-8 processing is accelerated in caspase-8:cFLIP$_L$ heterodimers, the activity of caspase-8 toward pro-apoptotic substrates (such as Bid and caspase-3) is greatly diminished, leading to inhibition of apoptosis.[36,47,49]

Figure 5. cFLIP$_L$ silencing results in increased FADD and RIPK1 recruitment to caspase-8/FADD/RIPK1 FADDosomes

(A) Schematic representation of membrane TRAIL receptor complex pull-down.

(B) HeLa cells (6 × 10^6 cells per treatment) were stimulated with 1.5 μg/mL of biotinylated TRAIL for the indicated periods of time in the presence or absence of Z-VAD-FMK (10 μM) followed by lysis of cells and incubation with streptavidin protein A/G beads for 5 h; captured complexes were analyzed by western blot.

(C) Schematic representation of cytosolic FADDosome complex immunoprecipitation (IP).

(D) Cell lysates after incubation with protein A/G agarose beads (from B) were subjected to IP with anti-caspase-8 antibody for 12 h; immunoprecipitated complexes were analyzed by western blot.

(E) HeLa cells were nucleofected with either non-targeting siRNA or cFLIP$_L$-targeting siRNA and, 48 h later, cells were treated with anti-Fas IgM (500 ng/mL) for the indicated times followed by IP of caspase-8. Caspase-8 IPs were then immunoblotted for the indicated proteins.

(F and G) HeLa cells were nucleofected with either non-targeting siRNA or cFLIP$_L$-targeting siRNA and, 48 h later, cells were treated with TRAIL for the indicated times followed by IP of caspase-8. Caspase-8 immunoprecipitates (F) and total cell lysates (G) were analyzed by SDS-PAGE and immunoblotted for the indicated proteins. See also Figure S5.

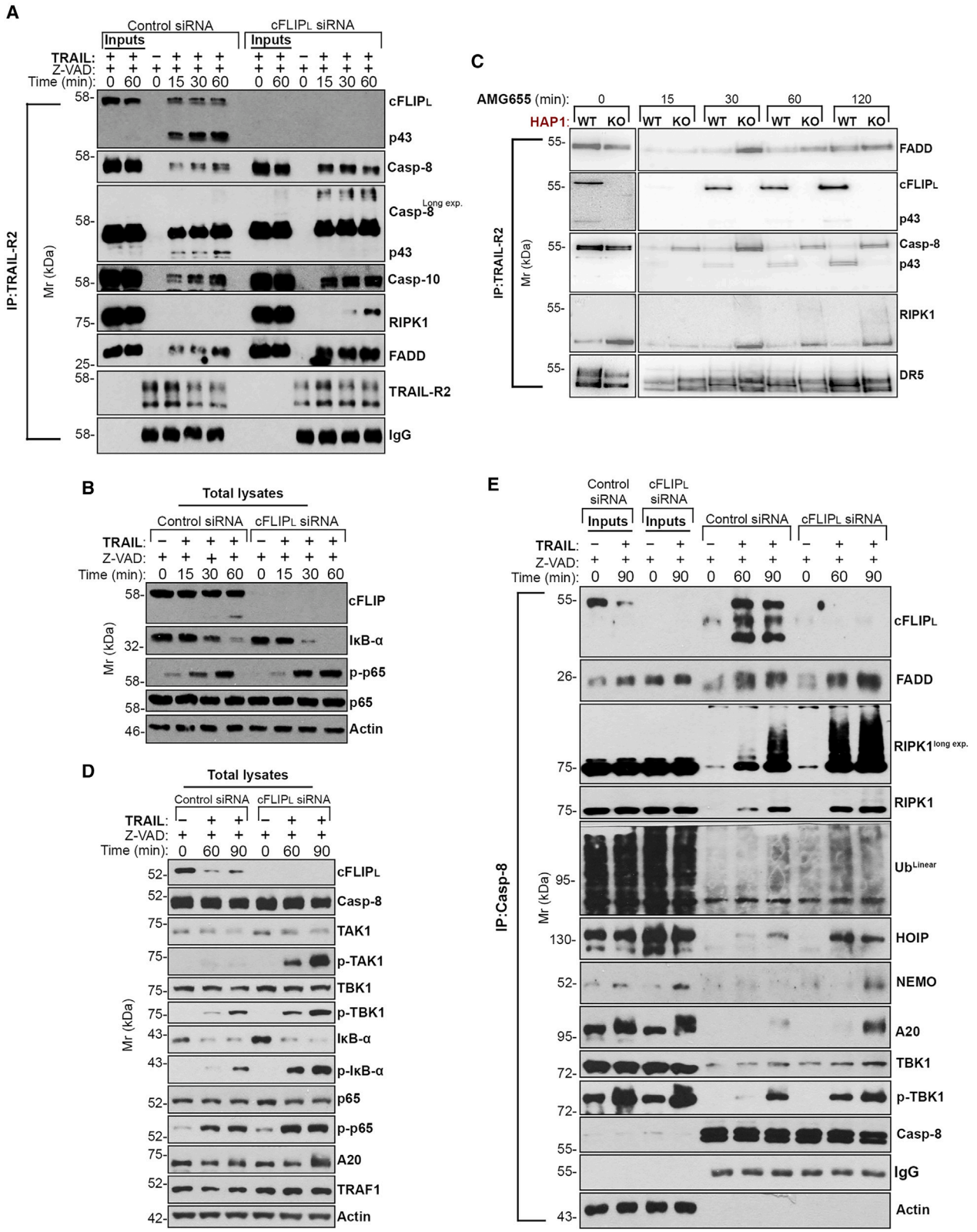

(legend on next page)

However, caspase-8:cFLIP$_L$ heterodimers exhibit protease activity toward RIPK1 and can cleave the latter, thereby restraining RIPK3-dependent necroptosis.[47,49] This also leads to the possibility that the diminished RIPK1-mediated NF-κB activation that is observed in the presence of cFLIP$_L$ could be due to enhanced cleavage of RIPK1 by capase-8:cFLIP$_L$ heterodimers. However, as we have shown (Figures 3A–3D), suppression of RIPK1 cleavage using poly-caspase inhibitors still led to greatly enhanced inflammatory cytokine production upon silencing of FLIP$_L$ expression, irrespective of RIPK1 cleavage status, demonstrating that the impact of cFLIP$_L$ on TRAIL- or Fas-mediated cytokine production can be uncoupled from RIPK1 proteolysis. In sharp contrast, loss of cFLIP$_L$ from FADDosome complexes led to robust increases in RIPK1 recruitment to the latter complexes, consistent with a mechanism whereby cFLIP$_L$ restrains NF-κB activation primarily through limiting the recruitment of FADD-RIPK1 to these complexes, or the formation of these complexes, due to the poor affinity of cFLIP$_L$ for FADD as compared with the high affinity of caspase-8 for the latter. Consistent with these observations, we have previously shown that caspase-8 plays an indispensable scaffold role for the formation of caspase-8/FADD/RIPK1 complexes to drive Fas- or TRAIL-induced cytokine production, demonstrating that neither caspase-10 nor cFLIP$_L$ can substitute for caspase-8 upon deletion or silencing of the latter.[10] Thus, despite the high sequence and structural similarity between caspase-8, cFLIP$_L$, and caspase-10, FADDosomes appear to have an obligate requirement for caspase-8 as the central scaffold protein.

The observations that cFLIP$_L$ acts as a potent suppressor of Fas- and TRAIL-induced inflammation raises the possibility that at least some of the effects of *cFLIP*/*CFLAR* loss *in vivo*, as reported in previous studies,[52–56] could be related to increased RIPK1-dependent inflammation as opposed to increased apoptosis. Deletion of *CFLAR* (cFLIP) or *CASP-8* is lethal[52,53]; however, the lethality seen due to loss of *CASP-8* can be rescued through concurrent deletion of RIPK3, indicating that *CASP-8*-associated lethality is due to excessive necroptosis.[52] In contrast, lethality associated with deletion of *CFLAR* was not corrected through deletion of *RIPK3* but could be rescued through deletion of *FADD* and *RIPK3* concurrently.[52] While the latter observation suggested that *CFLAR* loss is lethal due to excessive FADD-dependent capase-8 activation (leading to apoptosis), as well as RIPK1/RIPK3-dependent necroptosis, it is also possible that this phenotype could be related to excessive FADD/RIPK1-dependent inflammation. In agreement with the latter possibility, conditional deletion of *CFLAR* in the skin is lethal,[53] apparently due to excessive RIPK1-dependent autocrine TNF production, which results in excessive spontaneous apoptosis *in vitro* and *in vivo* due to the absence of cFLIP$_L$ to restrain caspse-8 activity.[53] Furthermore, a recent study demonstrated that, while concurrent deletion of *CFLAR* and *TNF* considerably ameliorated the skin phenotype associated with FLIP loss, a delayed inflammatory phenotype was still observed,[56] suggesting that loss of cFLIP also leads to excessive production of other FADD/RIPK1-dependent cytokines. Furthermore, conditional depletion of cFLIP in myeloid cells also results in enhanced inflammatory signaling *in vivo*.[55] Deletion of *CFLAR* in the dendritic cell (DC) compartment led to neutrophilia and splenomegaly, which correlated with enhanced p38^{MAPK} activation,[55] as we have also observed in the present study (Figures 3C–3E). *CFLAR*-knockout cDCs, plasmacytoid DCs, and bone marrow-derived DCs displayed enhanced production of TNF, IL-2, and granulocyte colony-stimulating factor (G-CSF) in response to Toll-like receptor (TLR) 4-, TLR2-, and dectin-1 receptor engagement, which was found to be independent of caspase-8 activity.[55] Thus multiple independent lines of evidence argue that loss of cFLIP *in vivo* results in enhanced inflammatory cytokine production. Interestingly, a recent study has also implicated cFLIP$_L$ as a suppressor of LPS-induced IL-1β production.[57] However, in the latter instance, loss of cFLIP resulted in enhanced complex II-associated caspase-8 activation, pyroptosis, and IL-1β release downstream. Thus, the role of cFLIP$_L$ in suppressing inflammation in the context of LPS-induced IL-1β production appears to be due to its conventional role as a regulator of caspase-8 activation, as opposed to the suppressive effects on RIPK1 recruitment we have uncovered here.

Limitations of this study

The schematic depicted in Figure 7J is a hypothetical model of caspase-8/FADD/RIPK1 FADDosomes based on the existing data relating to caspase-8 filaments formed downstream of death receptor engagement (complex I), which indicate that the latter filaments are composed of trimers of caspase-8 with a cap of FADD molecules at one end of the filament.[37,38] The FADDosome complex depicted in Figure 7J envisages a trimer of RIPK1 molecules recruited by a trimer of FADD molecules bound to one end of the caspase-8 trimeric filament. However, the true composition of FADDosome complexes awaits structural analysis and these complexes may be considerably larger than depicted. In the knockdown experiments depicted in Figures 7C and S6, the relatively modest effects of TRAF2 silencing on cytokine production could be related to the incomplete knockdown of TRAF2 observed in these experiments. Similarly, the modest effects of RIPK1 silencing on Fas- or TRAIL-induced cytokine production (Figures 4C, 4E, and 4F)

Figure 6. Elimination of cFLIP$_L$ leads to enhanced recruitment of RIPK1-associated inflammatory signaling mediators to FADDosomes

(A and B) HeLa cells were nucleofected with control oligo or siRNA targeted against cFLIP$_L$ and, 48 h later, cells were stimulated with TRAIL for the indicated periods of time in the presence of Z-VAD-FMK (10 μM) followed by preparation of cell lysates and IP of TRAIL-R2/DR5. TRAIL-R2 IPs (A) and total cell lysates (B) were then immunoblotted for the indicated proteins.

(C) HAP1 control and *CFLAR* KO cells were treated with anti-TRAIL-R2 agonistic antibody AMG655 for the indicated times. Captured membrane complexes were then analyzed by SDS-PAGE and immunoblotted for the indicated proteins.

(D and E) HeLa cells were nucleofected with control oligo or cFLIP$_L$-specific siRNA and, 48 h later, cells were stimulated with TRAIL for the indicated periods of time in the presence of Z-VAD-FMK (10 μM) followed by IP of caspase-8. Total cell lysates (D) and caspase-8 IPs (E) were then analyzed by SDS-PAGE and immunoblotted for RIPK1, linear Ub chains, and the indicated ubiquitin-binding proteins.

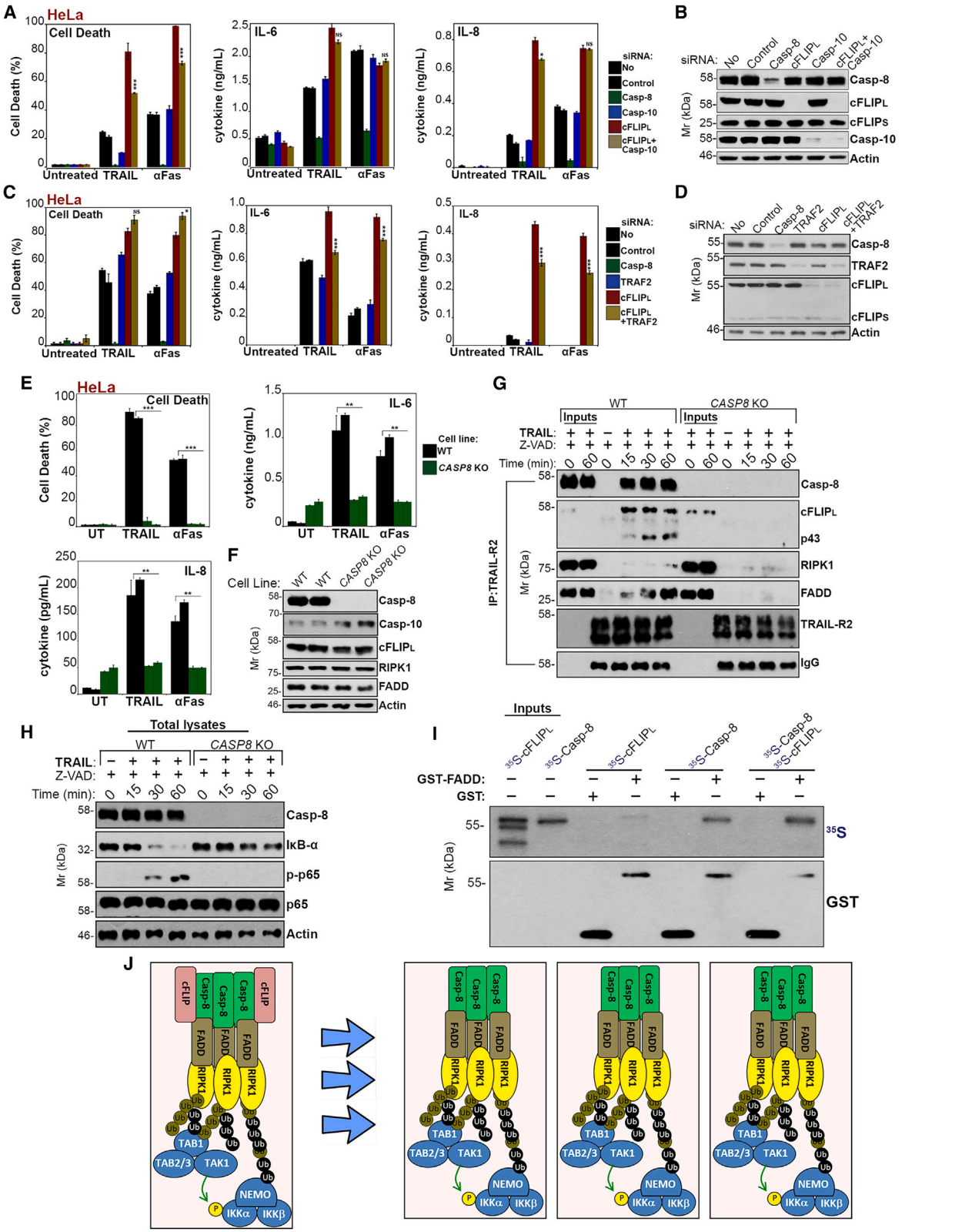

(legend on next page)

could also be related to incomplete RIPK1 knockdown or redundancy with TAK1.

In conclusion, here we have shown that cFLIP$_L$ acts as a bifunctional regulator of cell death and inflammation via distinct mechanisms. Although cFLIP$_L$ suppresses cell death through forming heterodimers with caspase-8, thereby restricting the protease activity of the latter to a narrow range of substrates, cFLIP$_L$ suppresses inflammation through blocking the formation of caspase-8/FADD/RIPK1 FADDosome complexes, thereby suppressing RIPK1 activation and inflammatory cytokine production downstream.

STAR★METHODS

Detailed methods are provided in the online version of this paper and include the following:

- KEY RESOURCES TABLE
- RESOURCE AVAILABILITY
  - Lead contact
  - Materials availability
  - Data and code availability
- EXPERIMENTAL MODEL AND STUDY PARTICIPANT DETAILS
  - Cell culture
- METHOD DETAILS
  - Apoptosis assays
  - Measurement of cytokines and chemokines
  - Western immunoblotting
  - DSS crosslinking
  - RNA interference
  - Protein overexpression
  - Expression and purification of GST-FADD and LZ-TRAIL
  - Biotinylation of LZ-TRAIL
  - GST-FADD pulldown assays
  - Coupled *in vitro* transcription/translation reactions
  - RNA preparation and RT-qPCR analysis
  - Immunoprecipitation of receptor and cytosolic complexes
  - Nuclear DNA staining
- QUANTIFICATION AND STATISTICAL ANALYSIS

SUPPLEMENTAL INFORMATION

Supplemental information can be found online at https://doi.org/10.1016/j.celrep.2023.113476.

ACKNOWLEDGMENTS

We thank Dr. Margot Thome (University of Lausanne) for provision of vFLIP expression plasmids and Dr. Domagoj Vucic (Genentech, USA) for the kind gift of BV6. The Martin laboratory is supported by grants from the Irish Research Council Laureate Award Programme (IRCLA/2019/133) and The European Research Council Advanced Grant Programme (DESTRESS).

AUTHOR CONTRIBUTIONS

P.D. designed and performed experiments, analyzed data, generated the figure panels, and wrote the figure legends. Z.N. and C.A.H. performed experiments. D.B.L. designed experiments. S.J.M. conceived the study, designed and analyzed experiments, supervised the study, and wrote the manuscript.

DECLARATION OF INTERESTS

The authors declare no competing interests.

Received: October 8, 2021
Revised: August 16, 2023
Accepted: November 3, 2023

REFERENCES

1. Ashkenazi, A., and Dixit, V.M. (1998). Death Receptors: Signaling and Modulation. Science *281*, 1305–1308.
2. Nagata, S. (1999). Fas ligand-induced apoptosis. Annu. Rev. Genet. *33*, 29–55.
3. Strasser, A., Jost, P.J., and Nagata, S. (2009). The many roles of FAS receptor signaling in the immune system. Immunity *30*, 180–192.
4. Cullen, S.P., and Martin, S.J. (2015). Fas and TRAIL 'death receptors' as initiators of inflammation: Implications for cancer. Semin. Cell Dev. Biol. *39*, 26–34.
5. von Karstedt, S., Montinaro, A., and Walczak, H. (2017). Exploring the TRAILs less travelled: TRAIL in cancer biology and therapy. Nat. Rev. Cancer *17*, 352–366.
6. Kreuz, S., Siegmund, D., Rumpf, J.J., Samel, D., Leverkus, M., Janssen, O., Häcker, G., Dittrich-Breiholz, O., Kracht, M., Scheurich, P., and Wajant, H. (2004). NFkappaB activation by Fas is mediated through FADD, caspase-8, and RIP and is inhibited by FLIP. J. Cell Biol. *166*, 369–380.

Figure 7. cFLIP$_L$ has a low affinity for FADD, compared with caspase-8, which limits recruitment of FADD-RIPK1 to FADDosomes

(A and C) HeLa cells were nucleofected with the indicated siRNAs and, 48 h later, cells were treated with TRAIL or anti-Fas for a further 18 h. Cytokine concentrations in culture supernatants were determined by ELISA and apoptosis was assessed based on cell morphology on counts of triplicate fields of at least 100 cells.

(B and D) Knockdown efficiency of cells treated in (A) or (C) was validated by western blotting.

(E) HeLa^{WT} and HeLa$^{CASP8-/-}$ cells were treated with TRAIL or anti-Fas for 18 h. Cytokine concentrations in supernatants were determined by ELISA.

(F) HeLa^{WT} and HeLa$^{CASP8-/-}$ cells were immunoblotted for the indicated proteins.

(G and H) HeLa^{WT} and HeLa$^{CASP8-/-}$ cells (6×10^6 cells per treatment) were stimulated with TRAIL in the presence of Z-VAD-FMK (10 μM) for the indicated times followed by IP with anti-TRAIL-R2/DR5 antibodies. TRAIL-R2 immunoprecipitates (G) and total lysates (H) were analyzed for the indicated proteins by western blot.

(I) *In vitro* transcribed/translated ^{35}S-labeled-cFLIP$_L$ and ^{35}S-labeled caspase-8 proteins were captured using recombinant GST or GST-FADD (2 μg per pull-down) conjugated to glutathione beads. After capture, complexes were subjected to SDS-PAGE and radiography analysis.

(J) Schematic representation of FADDosomes under conditions of high (left) or low (right) cFLIP$_L$ occupancy. However, where cFLIP$_L$ is abundant (left), caspase-8/cFLIP$_L$ heterodimers form, which suppresses caspase-8 protease activity to restrict apoptosis as well as suppressing the recruitment of FADD/RIPK1 due to the low affinity of cFLIP$_L$ for FADD, as compared with caspase-8. Thus, high cFLIP$_L$ levels suppress RIPK1-dependent NF-κB activation and inflammation. Error bars represent the mean ± SEM of triplicate cell counts from a representative experiment. Significance levels: ***$p < 0.0001$, **$p < 0.001$, *$p < 0.01$ by Student's t test. See also Figure S6.

7. Berg, D., Stühmer, T., Siegmund, D., Müller, N., Giner, T., Dittrich-Breiholz, O., Kracht, M., Bargou, R., and Wajant, H. (2009). Oligomerized tumor necrosis factor-related apoptosis inducing ligand strongly induces cell death in myeloma cells, but also activates proinflammatory signaling pathways. FEBS J. *276*, 6912–6927.

8. Kavuri, S.M., Geserick, P., Berg, D., Dimitrova, D.P., Feoktistova, M., Siegmund, D., Gollnick, H., Neumann, M., Wajant, H., and Leverkus, M. (2011). Cellular FLICE-inhibitory protein (cFLIP) isoforms block CD95- and TRAIL death receptor-induced gene induction irrespective of processing of caspase-8 or cFLIP in the death-inducing signaling complex. J. Biol. Chem. *286*, 16631–16646.

9. Cullen, S.P., Henry, C.M., Kearney, C.J., Logue, S.E., Feoktistova, M., Tynan, G.A., Lavelle, E.C., Leverkus, M., and Martin, S.J. (2013). Fas/CD95-Induced Chemokines Can Serve as "Find-Me" Signals for Apoptotic Cells. Mol. Cell *49*, 1034–1048.

10. Henry, C.M., and Martin, S.J. (2017). Caspase-8 Acts in a Non-enzymatic Role as a Scaffold for Assembly of a Pro-inflammatory "FADDosome" Complex upon TRAIL Stimulation. Molecular cell *65*, 715–729.e715.

11. Hartwig, T., Montinaro, A., von Karstedt, S., Sevko, A., Surinova, S., Chakravarthy, A., Taraborrelli, L., Draber, P., Lafont, E., Arce Vargas, F., et al. (2017). The TRAIL-Induced Cancer Secretome Promotes a Tumor-Supportive Immune Microenvironment via CCR2. Mol. Cell *65*, 730–742.e5.

12. Lafont, E., Kantari-Mimoun, C., Draber, P., De Miguel, D., Hartwig, T., Reichert, M., Kupka, S., Shimizu, Y., Taraborrelli, L., Spit, M., et al. (2017). The linear ubiquitin chain assembly complex regulates TRAIL-induced gene activation and cell death. The EMBO journal *36*, 1147–1166.

13. Siegmund, D., Lang, I., and Wajant, H. (2017). Cell death-independent activities of the death receptors CD95, TRAILR1, and TRAILR2. FEBS J. *284*, 1131–1159.

14. Sullivan, G.P., O'Connor, H., Henry, C.M., Davidovich, P., Clancy, D.M., Albert, M.L., Cullen, S.P., and Martin, S.J. (2020). TRAIL Receptors Serve as Stress-Associated Molecular Patterns to Promote ER-Stress-Induced Inflammation. Dev. Cell *52*, 714–730.e5.

15. Van Antwerp, D.J., Martin, S.J., Kafri, T., Green, D.R., and Verma, I.M. (1996). Suppression of TNF-alpha-induced apoptosis by NF-kappaB. Science *274*, 787–789.

16. Beg, A.A., and Baltimore, D. (1996). An essential role for NF-kappaB in preventing TNF-alpha-induced cell death. Science *274*, 782–784.

17. Kearney, C.J., Sheridan, C., Cullen, S.P., Tynan, G.A., Logue, S.E., Afonina, I.S., Vucic, D., Lavelle, E.C., and Martin, S.J. (2013). Inhibitor of apoptosis proteins (IAPs) and their antagonists regulate spontaneous and tumor necrosis factor (TNF)-induced proinflammatory cytokine and chemokine production. J. Biol. Chem. *288*, 4878–4890.

18. Varfolomeev, E., Blankenship, J.W., Wayson, S.M., Fedorova, A.V., Kayagaki, N., Garg, P., Zobel, K., Dynek, J.N., Elliott, L.O., Wallweber, H.J.A., et al. (2007). IAP antagonists induce autoubiquitination of c-IAPs, NF-kappaB activation, and TNFalpha-dependent apoptosis. Cell *131*, 669–681.

19. Vince, J.E., Wong, W.W.L., Khan, N., Feltham, R., Chau, D., Ahmed, A.U., Benetatos, C.A., Chunduru, S.K., Condon, S.M., McKinlay, M., et al. (2007). IAP antagonists target cIAP1 to induce TNFalpha-dependent apoptosis. Cell *131*, 682–693.

20. Boldin, M.P., Goncharov, T.M., Goltseve, Y.V., and Wallach, D. (1996). Involvement of MACH, a Novel MORT1/FADD-Interacting Protease, in Fas/APO-1- and TNF Receptor–Induced Cell Death. Cell *85*, 803–815.

21. Muzio, M., Chinnaiyan, A.M., Kischkel, F.C., O'Rourke, K., Shevchenko, A., Ni, J., Scaffidi, C., Bretz, J.D., Zhang, M., Gentz, R., et al. (1996). FLICE, a novel FADD-homologous ICE/CED-3-like protease, is recruited to the CD95 (Fas/APO-1) death–inducing signaling complex. Cell *85*, 817–827.

22. Afonina, I.S., Tynan, G.A., Logue, S.E., Cullen, S.P., Bots, M., Lüthi, A.U., Reeves, E.P., McElvaney, N.G., Medema, J.P., Lavelle, E.C., et al. (2011). Granzyme B-dependent proteolysis acts as a switch to enhance the proinflammatory activity of IL-1alpha. Mol. Cell *44*, 265–278.

23. Sprick, M.R., Weigand, M.A., Rieser, E., Rauch, C.T., Juo, P., Blenis, J., Krammer, P.H., and Walczak, H. (2000). FADD/MORT1 and caspase-8 are recruited to TRAIL receptors 1 and 2 and are essential for apoptosis mediated by TRAIL receptor 2. Immunity *12*, 599–609.

24. Kischkel, F.C., Lawrence, D.A., Chuntharapai, A., Schow, P., Kim, K.J., and Ashkenazi, A. (2000). Apo2L/TRAIL-dependent recruitment of endogenous FADD and caspase-8 to death receptors 4 and 5. Immunity *12*, 611–620.

25. Lavrik, I.N., Mock, T., Golks, A., Hoffmann, J.C., Baumann, S., and Krammer, P.H. (2008). CD95 stimulation results in the formation of a novel death effector domain protein-containing complex. J. Biol. Chem. *283*, 26401–26408.

26. Micheau, O., and Tschopp, J. (2003). Induction of TNF Receptor I-Mediated Apoptosis via Two Sequential Signaling Complexes. Cell *114*, 181–190.

27. Wajant, H. (2017). TRAIL- and TNF-induced signaling complexes-so similar yet so different. The EMBO journal *36*, 1117–1119.

28. Wang, L., Du, F., and Wang, X. (2008). TNF-alpha induces two distinct caspase-8 activation pathways. Cell *133*, 693–703.

29. Tenev, T., Bianchi, K., Darding, M., Broemer, M., Langlais, C., Wallberg, F., Zachariou, A., Lopez, J., MacFarlane, M., Cain, K., and Meier, P. (2011). The Ripoptosome, a signaling platform that assembles in response to genotoxic stress and loss of IAPs. Mol. Cell *43*, 432–448.

30. Feoktistova, M., Geserick, P., Kellert, B., Dimitrova, D.P., Langlais, C., Hupe, M., Cain, K., MacFarlane, M., Häcker, G., and Leverkus, M. (2011). cIAPs block Ripoptosome formation, a RIP1/caspase-8 containing intracellular cell death complex differentially regulated by cFLIP isoforms. Mol. Cell *43*, 449–463.

31. Tummers, B., Mari, L., Guy, C.S., Heckmann, B.L., Rodriguez, D.A., Rühl, S., Moretti, J., Crawford, J.C., Fitzgerald, P., Kanneganti, T.D., et al. (2020). Caspase-8-Dependent Inflammatory Responses Are Controlled by Its Adaptor, FADD, and Necroptosis. Immunity *52*, 994–1006.e8.

32. Irmler, M., Thome, M., Hahne, M., Schneider, P., Hofmann, K., Steiner, V., Bodmer, J.-L., Schröter, M., Burns, K., Mattmann, C., et al. (1997). Inhibition of death receptor signals by cellular FLIP. Nature *388*, 190–195.

33. Micheau, O., Thome, M., Schneider, P., Holler, N., Tschopp, J., Nicholson, D.W., Briand, C., and Grütter, M.G. (2002). The long form of FLIP is an activator of caspase-8 at the Fas death-inducing signaling complex. J. Biol. Chem. *277*, 45162–45171.

34. Dickens, L.S., Boyd, R.S., Jukes-Jones, R., Hughes, M.A., Robinson, G.L., Fairall, L., Schwabe, J.W.R., Cain, K., and Macfarlane, M. (2012). A death effector domain chain DISC model reveals a crucial role for caspase-8 chain assembly in mediating apoptotic cell death. Mol. Cell *47*, 291–305.

35. Schleich, K., Warnken, U., Fricker, N., Oztürk, S., Richter, P., Kammerer, K., Schnölzer, M., Krammer, P.H., and Lavrik, I.N. (2012). Stoichiometry of the CD95 Death-Inducing Signaling Complex: Experimental and Modeling Evidence for a Death Effector Domain Chain Model. Mol. Cell *47*, 306–319.

36. Hughes, M.A., Powley, I.R., Jukes-Jones, R., Horn, S., Feoktistova, M., Fairall, L., Schwabe, J.W.R., Leverkus, M., Cain, K., and MacFarlane, M. (2016). Co-operative and Hierarchical Binding of c-FLIP and Caspase-8: A Unified Model Defines How c-FLIP Isoforms Differentially Control Cell Fate. Mol. Cell *61*, 834–849.

37. Fu, T.-M., Li, Y., Lu, A., Li, Z., Vajjhala, P.R., Cruz, A.C., Srivastava, D.B., DiMaio, F., Penczek, P.A., Siegel, R.M., et al. (2016). Cryo-EM Structure of Caspase-8 Tandem DED Filament Reveals Assembly and Regulation Mechanisms of the Death-Inducing Signaling Complex. Mol. Cell *64*, 236–250.

38. Fox, J.L., Hughes, M.A., Meng, X., Sarnowska, N.A., Powley, I.R., Jukes-Jones, R., Dinsdale, D., Ragan, T.J., Fairall, L., Schwabe, J.W.R., et al. (2021). Cryo-EM structural analysis of FADD:Caspase-8 complexes defines the catalytic dimer architecture for co-ordinated control of cell fate. Nat. Commun. *12*, 819.

39. Majkut, J., Sgobba, M., Holohan, C., Crawford, N., Logan, A.E., Kerr, E., Higgins, C.A., Redmond, K.L., Riley, J.S., Stasik, I., et al. (2014). Differential affinity of FLIP and procaspase 8 for FADD's DED binding surfaces regulates DISC assembly. Nat. Commun. *5*, 3350.

40. Riley, J.S., Malik, A., Holohan, C., and Longley, D.B. (2015). DED or alive: assembly and regulation of the death effector domain complexes. Cell Death Dis. *6*, e1866.

41. Humphreys, L.M., Fox, J.P., Higgins, C.A., Majkut, J., Sessler, T., McLaughlin, K., McCann, C., Roberts, J.Z., Crawford, N.T., McDade, S.S., et al. (2020). A revised model of TRAIL-R2 DISC assembly explains how FLIP(L) can inhibit or promote apoptosis. EMBO Rep. *21*, e49254.

42. Chaudhary, P.M., Eby, M.T., Jasmin, A., Kumar, A., Liu, L., and Hood, L. (2000). Activation of the NF-kappaB pathway by caspase 8 and its homologs. Oncogene *19*, 4451–4460.

43. Hu, W.H., Johnson, H., and Shu, H.B. (2000). Activation of NF-kappaB by FADD, Casper, and caspase-8. J. Biol. Chem. *275*, 10838–10844.

44. Wajant, H., Haas, E., Schwenzer, R., Muhlenbeck, F., Kreuz, S., Schubert, G., Grell, M., Smith, C., and Scheurich, P. (2000). Inhibition of death receptor-mediated gene induction by a cycloheximide-sensitive factor occurs at the level of or upstream of Fas-associated death domain protein (FADD). J. Biol. Chem. *275*, 24357–24366.

45. Golks, A., Brenner, D., Krammer, P.H., and Lavrik, I.N. (2006). The c-FLIP-NH2 terminus (p22-FLIP) induces NF-kappaB activation. J. Exp. Med. *203*, 1295–1305.

46. Varfolomeev, E., Maecker, H., Sharp, D., Lawrence, D., Renz, M., Vucic, D., and Ashkenazi, A. (2005). Molecular determinants of kinase pathway activation by Apo2 ligand/tumor necrosis factor-related apoptosis-inducing ligand. J. Biol. Chem. *280*, 40599–40608.

47. Pop, C., Oberst, A., Drag, M., Van Raam, B.J., Riedl, S.J., Green, D.R., and Salvesen, G.S. (2011). FLIP(L) induces caspase 8 activity in the absence of interdomain caspase 8 cleavage and alters substrate specificity. Biochem. J. *433*, 447–457.

48. Lin, Y., Devin, A., Rodriguez, Y., and Liu, Z.G. (1999). Cleavage of the death domain kinase RIP by caspase-8 prompts TNF-induced apoptosis. Genes Dev. *13*, 2514–2526.

49. Oberst, A., Dillon, C.P., Weinlich, R., McCormick, L.L., Fitzgerald, P., Pop, C., Hakem, R., Salvesen, G.S., and Green, D.R. (2011). Catalytic activity of the caspase-8-FLIP(L) complex inhibits RIPK3-dependent necrosis. Nature *471*, 363–367.

50. Horn, S., Hughes, M.A., Schilling, R., Sticht, C., Tenev, T., Ploesser, M., Meier, P., Sprick, M.R., MacFarlane, M., and Leverkus, M. (2017). Caspase-10 Negatively Regulates Caspase-8-Mediated Cell Death, Switching the Response to CD95L in Favor of NF-κB Activation and Cell Survival. Cell Rep. *19*, 785–797.

51. Scaffidi, C., Schmitz, I., Krammer, P.H., and Peter, M.E. (1999). The role of c-FLIP in modulation of CD95-induced apoptosis. J. Biol. Chem. *274*, 1541–1548.

52. Dillon, C.P., Oberst, A., Weinlich, R., Janke, L.J., Kang, T.B., Ben-Moshe, T., Mak, T.W., Wallach, D., and Green, D.R. (2012). Survival function of the FADD-CASPASE-8-cFLIP(L) complex. Cell Rep. *1*, 401–407.

53. Panayotova-Dimitrova, D., Feoktistova, M., Ploesser, M., Kellert, B., Hupe, M., Horn, S., Makarov, R., Jensen, F., Porubsky, S., Schmieder, A., et al. (2013). cFLIP regulates skin homeostasis and protects against TNF-induced keratinocyte apoptosis. Cell Rep. *5*, 397–408.

54. Weinlich, R., Oberst, A., Dillon, C.P., Janke, L.J., Milasta, S., Lukens, J.R., Rodriguez, D.A., Gurung, P., Savage, C., Kanneganti, T.D., and Green, D.R. (2013). Protective roles for caspase-8 and cFLIP in adult homeostasis. Cell Rep. *5*, 340–348.

55. Wu, Y.J., Wu, Y.H., Mo, S.T., Hsiao, H.W., He, Y.W., and Lai, M.Z. (2015). Cellular FLIP Inhibits Myeloid Cell Activation by Suppressing Selective Innate Signaling. J. Immunol. *195*, 2612–2623. Baltimore, Md, 1950.

56. Feoktistova, M., Makarov, R., Leverkus, M., Yazdi, A.S., and Panayotova-Dimitrova, D. (2020). TNF Is Partially Required for Cell-Death-Triggered Skin Inflammation upon Acute Loss of cFLIP. Int. J. Mol. Sci. *21*, 8859.

57. Muendlein, H.I., Jetton, D., Connolly, W.M., Eidell, K.P., Magri, Z., Smirnova, I., and Poltorak, A. (2020). cFLIP(L) protects macrophages from LPS-induced pyroptosis via inhibition of complex II formation. Science *367*, 1379–1384.

STAR★METHODS

KEY RESOURCES TABLE

REAGENT or RESOURCE	SOURCE	IDENTIFIER
Antibodies		
Anti-A20 (A-12)	Santa-Cruz Biotechnology	#sc-166692
Anti-A20 (D13H3)	Cell Signaling	#5630
Anti-Actin (C4)	MP Biochemicals	#691001
Anti-BID (FL-195)	Santa-Cruz Biotechnology	#sc-11423
Anti-caspase-3 (cleaved)	Cell Signaling	#9661S
Anti-Caspase-8 (IP) (5D3)	MBL	#M058-3
Anti-Caspase-8 (IP)	R&D systems	#AF705
Anti-Caspase-8 (WB) (C15)	AdipoGen	#AG-20B-0057-C100
Anti-Caspase-10 (4C1)	MBL	#M059-3
Anti-cFLIP (7F10)	ENZO	#ALX-804-961-0100
Anti-cIAP1	Cell Signaling	#7065S
Anti-cIAP2	Cell Signaling	#3130S
Anti-CYLD (E−10)	Santa-Cruz Biotechnology	#sc-74435
Anti-DR4	Cell Signaling	#42533S
Anti-DR5 (IP)	R&D systems	#AF631
Anti-DR5 AMG655, Conatumumab (IP)	D. Longley	N/A
Anti-DR5 (WB)	Cell Signaling	#8074s
Anti-FADD	BD Transduction Laboratories	#610400
Anti-FADD (A66-2)	BD Transduction Laboratories	#556402
Anti-Fas (CH11)	Merck Sigma	#05-201
Anti-FLAG	Merck Sigma	#F7425
Anti-GST (B-14)	Santa-Cruz Biotechnology	#sc-138
Anti-GFP	Roche	#14717400
Anti-HIOP	R&D systems	#MAB8039
Anti-Iκβ-α	Cell Signaling	#9242S
Anti-p^{Ser32}-Iκβ-α (14D4)	Cell Signaling	#2859T
Anti-IKKγ	Cell Signaling	#2685S
Anti-p38	Cell Signaling	#9212s
Anti-p-p38	Cell Signaling	#4511s
Anti-p62	Santa-Cruz Biotechnology	#sc-28359
Anti-p65 (C-20)	Santa-Cruz Biotechnology	#sc-372
Anti-p^{Ser53}-p65 (93H1)	Cell Signaling	#3033
Anti-PARP	BD Transduction Laboratories	556594
Anti-RIPK1	BD Transduction Laboratories	#610459
Anti-RIPK1 (D94C12)	Cell Signaling	#3493S
Anti-TAK1	Cell Signaling	#5206S
Anti-*p*-TAK1 (90C7)	Cell Signaling	#4508S
Anti-TBK1 (D1B4)	Cell Signaling	#3504S
Anti-*p*-TBK1 (D52C2)	Cell Signaling	#5483S
Anti-TNF-α	R&D systems	#MAB601
Anti-TRAF1 (45D3)	Cell Signaling	#4715T
Anti-TRAF2 (C-20)	Santa-Cruz Biotechnology	#sc-876

(*Continued on next page*)

Continued

REAGENT or RESOURCE	SOURCE	IDENTIFIER
Anti-TRIF	Cell Signaling	#4596
Anti-Ubiquitin-K63 (D7A11)	Cell Signaling	#5621S
Anti-XIAP	BD Transduction Laboratories	#610763
Streptavidin-HRP	Cytiva	#RPN1231
Peroxidase conjugated AffiniPure Goat Anti-Mouse IgG (H + L)	Jackson Immunoresearch	#115-035-003
Peroxidase conjugated AffiniPure Goat Anti-Rabbit IgG (H + L)	Jackson Immunoresearch	#111-035-003
Peroxidase conjugated AffiniPure Goat Anti-Mouse IgG (L)	Jackson Immunoresearch	#115-035-174
Peroxidase conjugated AffiniPure Goat Anti-Mouse IgG (Fc)	Jackson Immunoresearch	#115-035-008
Peroxidase conjugated AffiniPure Goat Anti-Rabbit IgG (L)	Jackson Immunoresearch	#211-032-171 Lot 145158
IL-6 ELISA DuoSet	R&D systems	#DY206
IL-8 DuoSet	R&D systems	#DY208
CXCL1 DuoSet	R&D systems	#DY275
MCP1 DuoSet	R&D systems	#DY279
Chemicals, peptides, and recombinant proteins		
Z-VAD-FMK	Bachem	#N-1510.005
Emricasan	Sigma-Aldrich	#SML2227
BV6	Genentech	N/A
Cycloheximide	Sigma-Aldrich	C-7698
EZ-Link-Sulfo-NHS-Biotin	Thermo Scientific	A39256
Q-VD-OPh	Sigma-Aldrich	#SML0063-1MG
Recombinant IZ-TRAIL	Martin Laboratory	N/A
SuperKiller TRAIL	Adipogen	#AG-40T-0002-C020
Poly(I:C)	Sigma Aldrich	#P1530-100MG
TNF-α	Sigma Aldrich	#11371843001
Protein G-sepharose Fast Flow	Sigma Aldrich	#P3296
Glutathione Sepharose 4B	GE Healthcare	#17-0756-01
Streptavidin Sepharose	GE Healthcare	#17-5113-01
Ni-NTA	Expedeon	ANN0010
PR619	Sigma Aldrich	#SML0430
Ampicillin	Sigma Aldrich	#A9518
Kanamycin	Sigma Aldrich	#60615
cOmpleteTM protease inhibitor cocktail	Roche	#04693116001
Phosphatase inhibitor cocktail PhosSTOP	Roche	#04906845001
TnT Quick Coupled Transcription	Promega	#L1170
Amplify	GE Healthcare	#NAMP100V
Disuccinimidyl suberate (DSS)	Thermo Scientific	#21655
BisBenzimide H 33342 trihydrochloride (DAPI)	Sigma-Aldrich	#B2261
Pierce Rapid Gold BCA Protein Assay Kit	Thermo Scientific	#A53225
RNeasy Kit	Qiagen	#74104
QuantiTect RT KIT	Qiagen	#205311
Luna Universal qPCR Master Mix	NEB	#M3003L
Lipofectamine 3000	Invitrogen	L3000-015

(*Continued on next page*)

Continued

REAGENT or RESOURCE	SOURCE	IDENTIFIER
Experimental models: Cell lines		
Human cervical cancer HeLa	Martin Laboratory	N/A
Human colon cancer HT-29	Martin Laboratory	N/A
Human colon cancer HCT-116	Martin Laboratory	N/A
Transformed keratinocytes HaCaT	Martin Laboratory	N/A
Human lung cancer A549	A. Budanov	N/A
HeLa *CASP8* KO	Martin Laboratory	Henry and Martin 2017[10]
Human chronic myeloid leukemia HAP1	D. Longley	Humphreys et al. 2020[41]
HAP1 *CFLAR* KO	D. Longley	Humphreys et al. 2020[41]
Bacteria: *E.Coli* DH5α	Martin Laboratory	N/A
Bacteria: *E.Coli* BL21 DE3	Martin Laboratory	N/A
Oligonucleotides		
Oligonucleotides used in this study are listed in Table S1	This paper	N/A
Recombinant DNA		
Plasmid: pcDNA.3	Martin Laboratory	N/A
Plasmid: pcDNA.3-caspase-8	Martin Laboratory	Henry and Martin 2017[10]
Plasmid: pcDNA.3-caspase-8-C360A	Martin Laboratory	Henry and Martin 2017[10]
Plasmid: pcDNA.6-cFLIPL-Myc	Marion Mc Farlaine	N/A
Plasmid: pAAV-eGFP	Martin Laboratory	N/A
Plasmid: pCR3-FLAG-MC159	Margot Thome	N/A
Plasmid: pCR3-FLAG-MC160	Margot Thome	N/A
Plasmid: pET28a-IZ-TRAIL	H. Walczak	N/A
Plasmid: pGex-GST	Martin Laboratory	N/A
Plasmid: pGex-GST-FADD	Martin Laboratory	N/A
Software and algorithms		
KaleidaGraph Version 5.0	Synergy Software	#604463
Adobe InDesign CS6	Adobe	N/A
Adobe Photoshop CS6	Adobe	N/A
Microsoft Office	Microsoft	N/A
ImageJ 1.53k	Wayne Rasband	N/A
PyMol	Christoph Gohlke, University of California, Irvine	N/A

RESOURCE AVAILABILITY

Lead contact

Further information and requests should be directed to and will be fulfilled or facilitated by the lead contact Seamus J. Martin (martinsj@tcd.ie).

Materials availability

Cell lines and plasmids used in this study are available upon request from the lead contact.

Data and code availability

- The data supporting the findings of this study are available within the article and its supplementary materials. Data reported in this paper can be shared by the lead contact upon request.
- This paper does not report original code.
- Any additional information required to reanalyze the data reported in this paper is available from the lead contact upon request.

EXPERIMENTAL MODEL AND STUDY PARTICIPANT DETAILS

Cell culture

All cell lines except HAP1 (obtained from the Longley laboratory, Center for Cancer Research and Cell Biology, Queen's University Belfast) were obtained from the Molecular Cell Biology laboratory, Trinity College Dublin. HeLa, HCT-116 cells were cultured in RPMI media, supplemented with 5% fetal calf serum (FCS). A549, HT-29 and HaCaT cells were cultured in DMEM supplemented with 10% FCS, HAP1 cells were cultured in IMDM medium supplemented with 10% FCS. For experimentation, cells were plated at a density of 1–2 x 10^5 cells/well in 6-well plates and cultured for a further 24 h before treatment.

METHOD DETAILS

Apoptosis assays

Cells were plated at 2 x 10^5 cells/well in 6-well plates and treated 24 h later with TRAIL, αFas, TNFα or poly(I:C) for the indicated times prior to enumeration of apoptosis based on cell morphology (cell rounding, detachment from the plate, nuclear condensation and presence of apoptotic bodies). A minimum of 300 cells were counted in each treatment. Alternatively, cell death was quantified using Annexin V/PI staining analyzed by flow cytometry. In brief, the assay is based on a 15 min incubation of cells in a solution containing 1 mM $CaCl_2$, 1 μg/mL annexin V-FITC and 10 μg/mL of PI.

Measurement of cytokines and chemokines

After treatment, cell culture supernatants were collected and clarified by centrifugation for 5 min at 2500 g. Cytokines and chemokines were measured from clarified cell culture supernatants using specific ELISA kits obtained from R&D Systems. Each assay was repeated a minimum of three times and all cytokine assays were carried out using triplicate samples from each culture.

Western immunoblotting

Cell lysates were prepared using SDS-PAGE loading buffer and were electrophoresed on 10–15% SDS-PAGE gels followed by transfer onto nitrocellulose membranes at 40 mA overnight, followed by probing membranes with specific primary and secondary antibodies to reveal specific proteins. Protein levels were normalized using Pierce Rapid Gold BCA Protein Assay Kit.

DSS crosslinking

HeLa cells (8x10^6) were transfected with either non-targeting or cFLIPL siRNAs, and after 48 h were treated with TRAIL for indicated time periods. After TRAIL treatment cells were washed three times with DPBS and lysed with 1 mL of "DSS-lysis buffer" (30 mM HEPES pH 7.4, 150 mM NaCl, 2 mM EDTA, 1% Triton X-100, 10% glycerol) for 1 h at 4°C. Lysates were pelleted twice at 15000 g for 5 or 10 min at 4°C. Lysate components were crosslinked at room temperature with 1 M DSS (0.1 mM final) for the indicated times. Reaction was quenched with 1 M TRIS-HCl pH 7.4 (50 mM final) for 30 min at room temperature. Crosslinked products were examined by Western blot.

RNA interference

Cells (10^6 per nucleofection) were nucleofected with 2 μM of each siRNA (see key resources table for oligo details) in nucleofection buffer (5 mM KCl, 15 mM $MgCl_2$, 20 mM HEPES, 150 mM Na_2HPO_4 pH 7.2) using Amaxa Nucleofector (program I-013 for HeLa, D-032 for HCT-116, W-17 for HT-29, X-001 for A549 and U-020 for HaCaT cells). Nucleofected cells were plated in 6-well plates (2x10^5 cells/well) and 48 h after nucleofection cells were stimulated as indicated.

Protein overexpression

In 6-well format 2x10^5 HeLa$^{CASP8-/-}$ cells were transfected with 300 ng of plasmid encoding catalytically mutant caspase-8^{C360A} along with 300 and 150 ng of cFLIP-L and vFLIP constructs (MC159 and MC160). pDNA amounts were normalized with empty pcDNA.3 vector. pAAV-eGFP was used to monitor transfection efficiency. Lipofectamine 3000 was used to deliver plasmid DNA.

Expression and purification of GST-FADD and LZ-TRAIL

E.Coli Rosetta (DE3) strain was transformed with pGEX-GST-FADD plasmid encoding full length FADD protein or empty pGEX-GST vector. The following day, well-defined colonies were picked and inoculated into 3 mL LB broth and incubated overnight at 37°C at 280–300 rpm. 2.5 mL of the overnight starter culture was then added to 250 mL LB to achieve and OD^{600} of 0.1 and then grow to OD^{600} of 0.4, followed by addition of IPTG to a final concentration of 100 μM and incubated for 3 h at 37°C. Bacteria were lysed by sonication and protein was captured using glutathione immobilized agarose beads. Leucine Zipper-(LZ)-TRAIL synthesis was induced from pET28a plasmid with 100 μM IPTG for 3 h at room temperature; induced protein was captured on Ni-NTA beads and eluted by PBS containing 1 mM imidazole. Protein purity and concentration was determined by SDS-PAGE, followed by Coomassie blue staining.

Biotinylation of LZ-TRAIL

Leucine Zipper-(LZ)-TRAIL was biotinylated with 20X molar excess of EZ-Link-Sulfo-NHS-Biotin for 30 min at room temperature in LZ-TRAIL elution buffer. Excess of biotin-tag was neutralized with 1 M Tris-HCl pH 7.5 for 10 min at room temperature. TRAIL biotinylation was confirmed by western blotting.

GST-FADD pulldown assays

In vitro translated[35][S]-labeled proteins were captured from 300 μL volume of "GST capture buffer" (in the presence of 50 mM NaCl) for 3 h at 4°C with 2 μg of GST or GST-FADD. After GST capture, beads were collected by centrifugation (2 min at 1000 g) and one wash with the same buffer was performed. Samples were eluted from beads in 40 μL of SDS lysis buffer and analyzed by SDS-PAGE followed by overnight exposure of dried gels to X-ray films at −80°C.

Coupled *in vitro* transcription/translation reactions

In vitro transcription/translation reactions were carried out for 2 h at 30°C using 1 μg of purified plasmids (pcDNA.3-caspase-8 and pcDNA.6-cFLIP-Long) added to a rabbit reticulocyte lysate system (Promega). *In vitro* translation efficiency was evaluated by running samples on SDS-PAGE, followed by fixation of gels (45% H_2O, 45% MeOH, 10% HOAc), incubation with (Amplify), followed by drying of gels for 2 h at 80°C and exposing to X-ray film at −80°C.

RNA preparation and RT-qPCR analysis

HeLa (5×10^5) cells were seeded in 6-well plates. The following day cells were treated, as described, and then total RNA was isolated using the Qiagen RNeasy kit and normalized before reverse transcription PCR using Qiagen QuantiTect RT kit. The resulting cDNA was used to seed real-time qPCR reactions and relative mRNA expression levels were determined by NEB SYBR Green I detection chemistry on an Applied Biosystems QuantStudio 3 RT-PCR system. RPO was used as the control normalizer for fold-change in mRNA expression. Error bars indicate standard deviation of triplicate qPCR data.

Immunoprecipitation of receptor and cytosolic complexes

HeLa cells (8×10^6 per treatment) were reverse treated with TRAIL or αFas for the indicated times. After treatment, cells were washed three times with DPBS and lysed with 1 mL of "IP-lysis buffer" (30 mM Tris-HCl pH 7.4, 150 mM NaCl, 2 mM EDTA, 1% Triton X-100, 10% Glycerol, cOmplete protease inhibitor cocktail and 10 μM DUB inhibitor PR619) for 1h at 4°C. Lysates were pelleted twice at 15000 g for 5 and 10 min at 4°C. Lysates were clarified with 15μL of protein G Sepharose beads for 1 h at 4°C. Clarified lysates were used as input samples. To the clarified lysates 20 μL of beads and 2 μg of anti-TRAIL-R2 or anti-caspase-8 antibodies were added and capture of the complexes continued overnight at 4°C. After capture beads were collected by centrifugation (2 min at 1000 g) and washed three times with 1.5 mL of "IP-lysis buffer" (450 mM NaCl). For sequential IP, receptor complexes were first captured from lysates by streptavidin Sepharose beads for 5h at 4C followed by capture of cytosolic complexes by anti-caspse-8 antibody for 12 h at 4°C. In each case samples were eluted from beads with 60 μL of SDS lysis buffer.

Nuclear DNA staining

All procedures were carried out at room temperature. HeLa cells at 2×10^5 cells/well in 6-well plates were then washed twice with DPBS and consequently stained for 30 min at room temperature with 10 μg/mL solution of Hoechst in DPBS solution. Pictures were taken using Olympus IX71 Microscope and further processed using ImageJ.

QUANTIFICATION AND STATISTICAL ANALYSIS

Error bars are represented as mean ± SEM. Statistical significance was calculated by Student's T test. Statistical tests were performed in Microsoft Excel using the TTEST function. Bar graphs were plotted as mean ± SDM and statistical significance was denoted as follows: *** = $p < 0.001$, ** = $p < 0.01$, * = $p < 0.05$, NS, not significant.